NICA

Nuclotron-based
Ion Collider fAcility

Resonance production and reconstruction in the MPD at NICA

Mikhail Malaev, Viktor Riabov

PNPI

Outline

- Motivation for resonance studies
- Experimental background
- Prospects for the MPD at NICA
- Resonance reconstruction – first look

Motivation

- A huge variety of resonances in the PDG
- Some of the resonances are copiously produced in pp/pA/AA collisions, well defined in the PDG (mass, width, decay channels and BRs), experimentally measurable at top multiplicities:
- Resonances differ by lifetime, mass and quark content → probe reaction dynamics and particle production mechanisms in different collision systems

$\rho(770)$	$K^*(892)^0$	$K^*(892)^+$	$\phi(1020)$	$\Sigma(1385)^\pm$	$\Lambda(1520)$	$\Xi(1530)$
$\frac{u\bar{u}+d\bar{d}}{\sqrt{2}}$	$d\bar{s}$	$u\bar{s}$	$s\bar{s}$	uus dds	uds	uss

Particle	Mass (MeV/c^2)	Width (MeV/c^2)	Decay	BR (%)
ρ^0	770	150	$\pi^+\pi^-$	100
$K^{*\pm}$	892	50.3	$\pi^\pm K_s$	33.3
K^{*0}	896	47.3	$\pi^- K^+$	66.7
ϕ	1019	4.27	K^+K^-	48.9
Σ^{*+}	1383	36	$\pi^+\Lambda$	87
Σ^{*-}	1387	39.4	$\pi^-\Lambda$	87
$\Lambda(1520)$	1520	15.7	K^-p	22.5
Ξ^{*0}	1532	9.1	$\pi^+\Xi^-$	66.7

Medium modifications

- Short lifetimes: → chiral symmetry restoration: mass/width modifications
  → hadronic phase: lifetime, density

- Reconstructed resonance yields in heavy ion collisions are defined by:
  - ✓ resonance yields at chemical freeze-out
  - ✓ hadronic processes between chemical and kinetic freeze-outs:

    rescattering: daughter particles undergo elastic scattering or pseudo-elastic scattering through a different resonance → parent particle is not reconstructed → loss of signal

    regeneration: pseudo-elastic scattering of decay products ($\pi K \rightarrow K^{*0}$, $KK \rightarrow \phi$ etc.) → increased yields

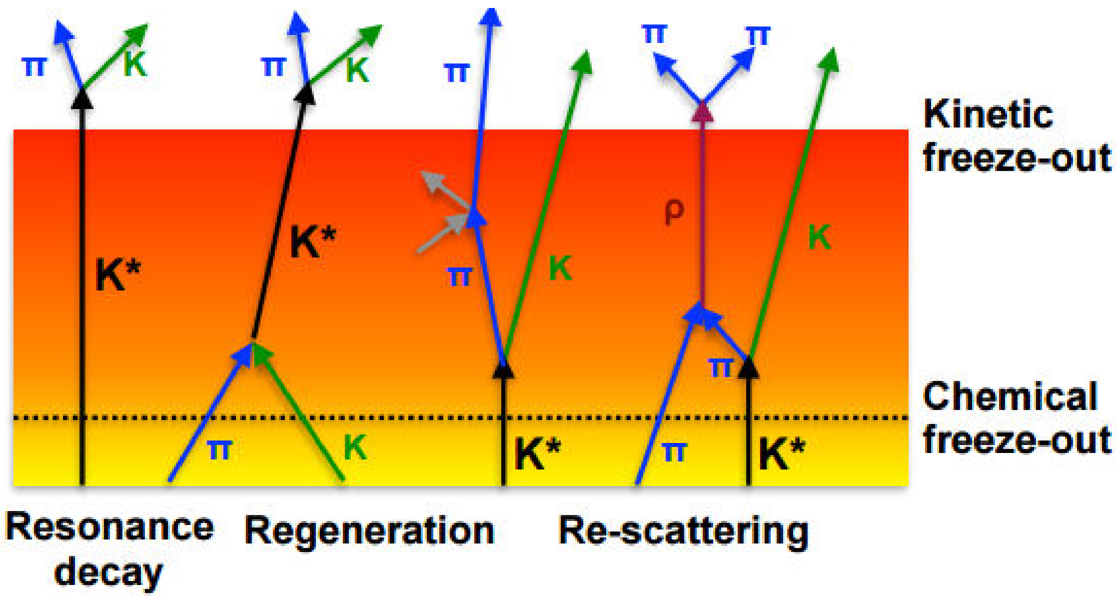

Hadronic phase

- Cumulative effect of the hadronic processes depends on:
  - ✓ lifetime and density of the hadronic phase
  - ✓ resonance lifetime and scattering cross sections (type of daughter particles)
- UrQMD: rescattering and regeneration are most important at low momenta → focus is on low p_T measurements

- Resonances with lifetimes comparable to that of the fireball are well suited to study properties of the hadronic phase

	$\rho(770)$	**$K^*(892)$**	**$\Sigma(1385)$**	**$\Lambda(1520)$**	**$\Xi(1530)$**	**$\phi(1020)$**
$c\tau$ (fm/c)	1.3	4.2	5.5	12.7	21.7	46.2
$\sigma_{rescatt}$	$\sigma_\pi\sigma_\pi$	$\sigma_\pi\sigma_K$	$\sigma_\pi\sigma_\Lambda$	$\sigma_K\sigma_p$	$\sigma_\pi\sigma_\Xi$	$\sigma_K\sigma_K$

Particle ratios at $\sqrt{s_{NN}}$ = 20-2760 GeV

increasing lifetime ⟶

	ρ(770)	K*(892)	Σ(1385)	Λ(1520)	Ξ(1530)	ϕ(1020)
cτ (fm/c)	1.3	4.2	5.5	12.7	21.7	46.2
$\sigma_{rescatt}$	$\sigma_\pi\sigma_\pi$	$\sigma_\pi\sigma_K$	$\sigma_\pi\sigma_\Lambda$	$\sigma_K\sigma_p$	$\sigma_\pi\sigma_\Xi$	$\sigma_K\sigma_K$

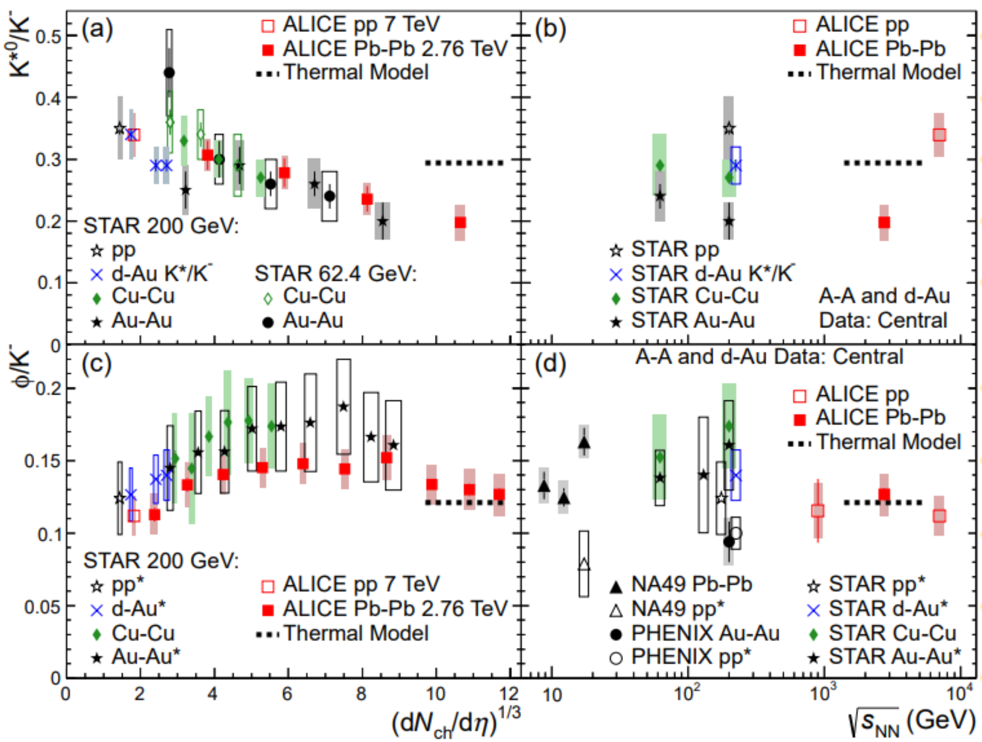

- Particle ratios show very weak energy dependence in a wide range $\sqrt{s_{NN}}$ = 20-2760 GeV

- ϕ/K:
  - ✓ no strong centrality dependence
  - ✓ consistent for pp, pA and AA
  - ✓ consistent with thermal models (Andronic et al., J. Phys.G38(2011) 124081)

- K^{*0}/K:
  - ✓ significant suppression going from pp to central AA collisions
  - ✓ Central AA results are inconsistent with thermal models

ALICE results in CERN Courier

CERN Courier July/August 2017

News

ALICE zooms in on evolution of the quark–gluon plasma

The precise particle-identification and momentum-measurement capabilities of the ALICE experiment allow researchers to reconstruct a variety of short-lived particles or resonances in heavy-ion collisions. These serve as a probe for in-medium effects during the last stages of evolution of the quark–gluon plasma (QGP). Recently, the ALICE collaboration has made a precise measurement of the yields (number of particles per event) of two such resonances: $K^*(892)^0$ and $\phi(1020)$. Both have similar masses and the same spin, and both are neutral strange mesons, yet their lifetimes differ by a factor of 10 (4.16±0.05 fm/c for K^{*0}, and 46.3±0.4 fm/c for ϕ).

The shorter lifetime of the K^{*0} means that it decays within the medium, enabling its decay products (π and K) to re-scatter with other hadrons. This would be expected to inhibit the reconstruction of the parent K^{*0}, but the π and K in the medium may also scatter into a K^{*0} resonance state, and the interplay of these two competing re-scattering and regeneration processes becomes relevant for determining the K^{*0} yield. The processes depend on the time interval between chemical freeze-out (vanishing inelastic collisions) and kinetic freeze-out (vanishing elastic collisions), in addition to the source size and the interaction cross-sections of the daughter hadrons. In

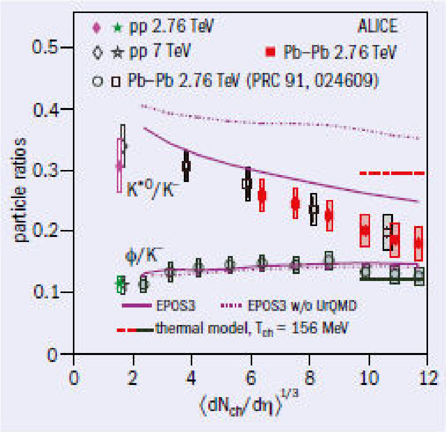

Ratio of K^{*0} and ϕ yields to charged-kaon yields at midrapidity for Pb–Pb and pp collisions as a function of charged-particle pseudorapidity density at midrapidity $(dN_{ch}/d\eta)^{1/3}$, which is related to the final-state freeze-out geometry of the system. Also shown are corresponding results from models with and without re-scattering.

contrast, due to the longer lifetime of the ϕ meson, both the re-scattering and regeneration effects are expected to be negligible.

Using lead–lead collision data recorded at an energy of 2.76 TeV, ALICE observed that the ratio K^{*0}/K^- decreases as a function of system size (see figure). In small impact-parameter collisions, the ratio is significantly less than in proton–proton collisions and models without re-scattering effects. In contrast, no such suppression was observed in the ϕ/K^- ratio. This measurement thus suggests the existence of re-scattering effects on resonances in the last stages of heavy-ion collisions at LHC energies. Furthermore, the suppression of K^{*0} yields can be used to obtain the time difference between the chemical and the kinetic freeze-out of the system.

On the other hand, at higher momenta ($p_T > 8$ GeV/c), these resonances were suppressed with respect to proton–proton collisions by similar amounts. The magnitude of this suppression for K^{*0} and ϕ mesons was also found to be similar to the suppression for pions, kaons, protons and D mesons. The striking independence of this suppression on particle mass, baryon number and the quark-flavour content of the hadron puts a stringent constraint on models dealing with particle-production mechanisms, fragmentation processes and parton energy loss in the QGP medium.

In future, it will be important to perform such measurements for high-multiplicity events in pp collisions at the LHC.

• Further reading

ALICE Collaboration 2017 *Phys. Rev. C.* 95 064606.

Particle ratios, ρ/π at $\sqrt{s_{NN}}$ = 2.76 TeV

arXiv:1805.04365

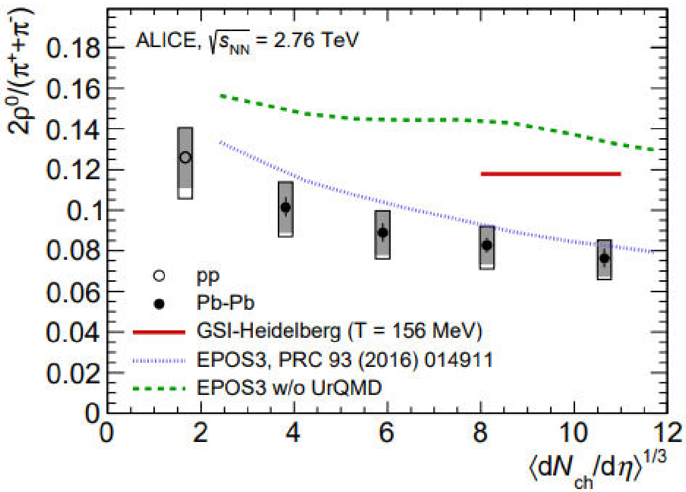

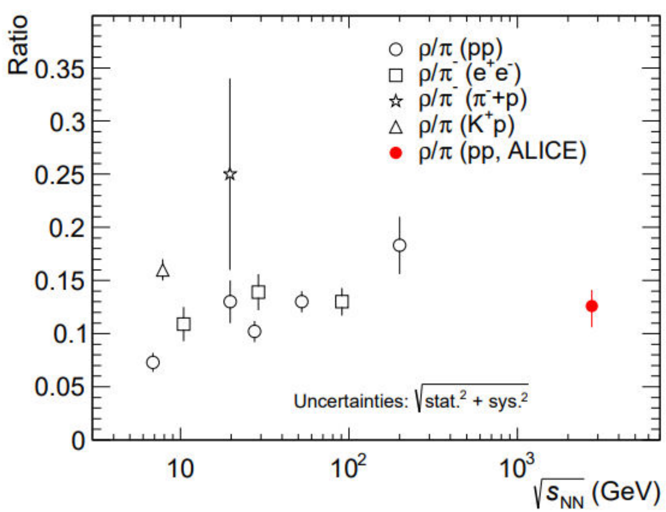

increasing lifetime →

	ρ(770)	K*(892)	Σ(1385)	Λ(1520)	Ξ(1530)	φ(1020)
cτ (fm/c)	1.3	4.2	5.5	12.7	21.7	46.2
$\sigma_{rescatt}$	$\sigma_\pi\sigma_\pi$	$\sigma_\pi\sigma_K$	$\sigma_\pi\sigma_\Lambda$	$\sigma_K\sigma_p$	$\sigma_\pi\sigma_\Xi$	$\sigma_K\sigma_K$

- ρ/π:
  - ✓ suppression from pp to central Pb-Pb
  - ✓ central Pb-Pb is inconsistent with thermal models
  - ✓ reproduced by EPOS3 with UrQMD

- Ratio in elementary collisions does not depend on collision energy, $\sqrt{s}$ > 10 GeV, within uncertainties

Z. Phys., vol. C61, 1994.
Phys. Lett., vol. B158, 1985.
Z. Phys., vol. C72, 1996.
Phys. Lett., vol. 48B, 1974.
Phys. Lett., vol. B60, 1976.
Z. Phys., vol. C50, 1991.
Z. Phys., vol. C9, 1981.
Nucl. Phys., vol. B176, 1980.
Phys. Lett., vol. B56, 1975.

Particle ratios, Λ^*/Λ at $\sqrt{s_{NN}}$ = 200-2760 GeV

arXiv:1805.04361

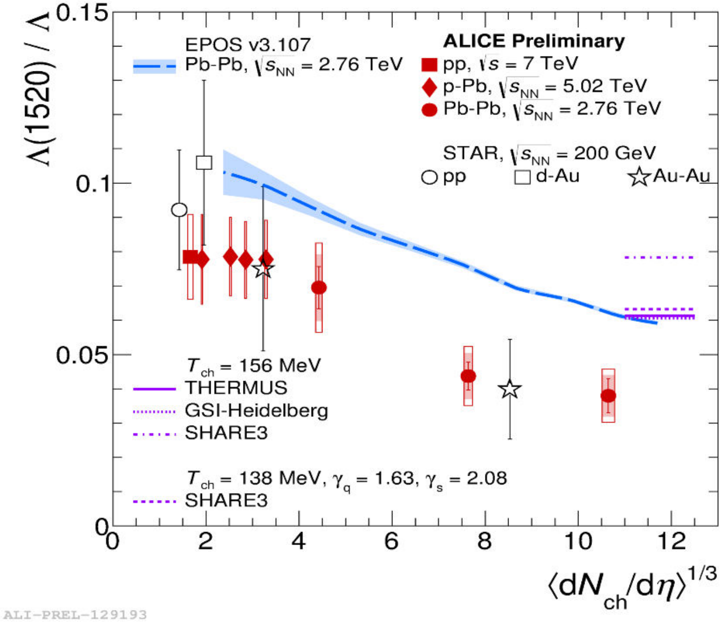

increasing lifetime →

	ρ(770)	K^*(892)	Σ(1385)	Λ(1520)	Ξ(1530)	φ(1020)
cτ (fm/c)	1.3	4.2	5.5	12.7	21.7	46.2
$\sigma_{rescatt}$	$\sigma_\pi\sigma_\pi$	$\sigma_\pi\sigma_K$	$\sigma_\pi\sigma_\Lambda$	$\sigma_K\sigma_p$	$\sigma_\pi\sigma_\Xi$	$\sigma_K\sigma_K$

- Λ^*/Λ:
  - ✓ suppression from pp to central Pb-Pb
  - ✓ central Pb-Pb is inconsistent with thermal models
  - ✓ qualitatively reproduced by EPOS3 with UrQMD
- Ratios in pp, p-A and A-A do not show strong dependence on collision energy, $\sqrt{s}$ = 0.2–5.02 TeV

Particle ratios, Ξ^*/Ξ at $\sqrt{s_{NN}}$ = 2.76 TeV

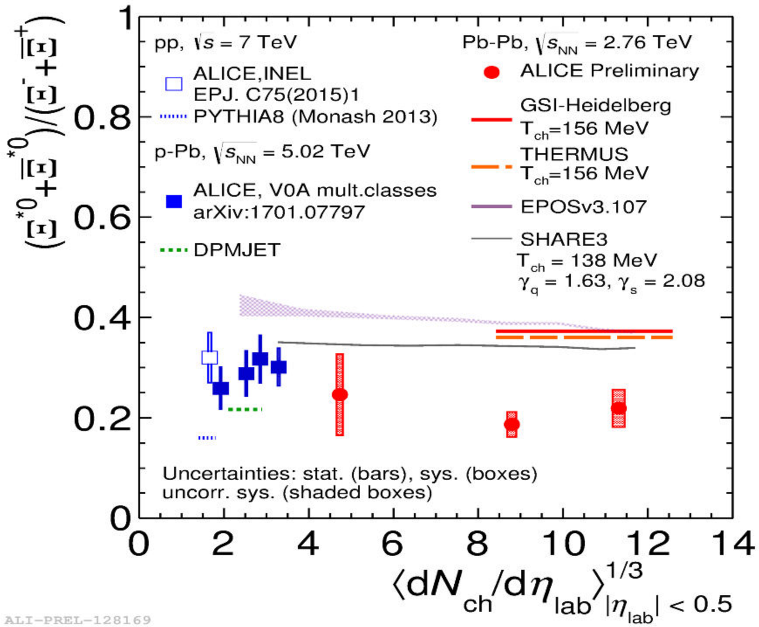

increasing lifetime ⟶

	$\rho(770)$	$K^*(892)$	$\Sigma(1385)$	$\Lambda(1520)$	$\Xi(1530)$	$\phi(1020)$
$c\tau$ (fm/c)	1.3	4.2	5.5	12.7	21.7	46.2
$\sigma_{rescatt}$	$\sigma_\pi\sigma_\pi$	$\sigma_\pi\sigma_K$	$\sigma_\pi\sigma_\Lambda$	$\sigma_K\sigma_p$	$\sigma_\pi\sigma_\Xi$	$\sigma_K\sigma_K$

- Ξ^*/Ξ:
  - ✓ no multiplicity dependence in pp, p-Pb
  - ✓ hint of suppression in central Pb-Pb, systematic uncertainties are to be reduced
  - ✓ models do not predict significant multiplicity dependence of the ratio
  - ✓ thermal models overestimate the ratio in Pb-Pb

Experimental summary

increasing lifetime ⟶

	ρ(770)	K*(892)	Λ(1520)	Ξ(1530)	ϕ(1020)
cτ (fm/c)	1.3	4.2	12.7	21.7	46.2
$\sigma_{rescatt}$	$\sigma_\pi\sigma_\pi$	$\sigma_\pi\sigma_K$	$\sigma_K\sigma_p$	$\sigma_\pi\sigma_\Xi$	$\sigma_K\sigma_K$

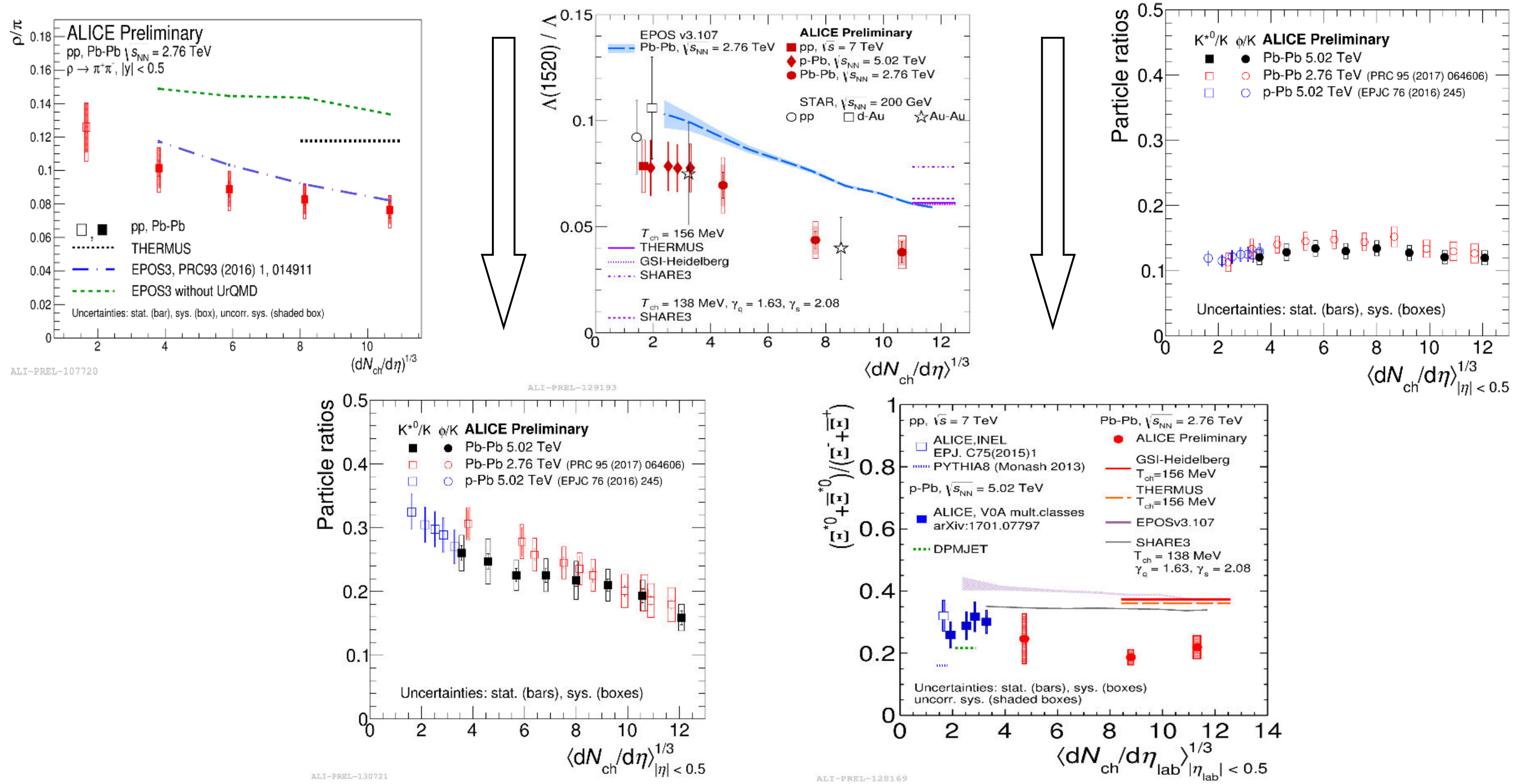

- Results support the existence of a hadronic phase long enough to cause a significant reduction of the reconstructed yields of short lived resonances
- Lower limit for the lifetime of the hadronic phase, τ > 2 fm/*c*

G. Torrieri and J. Rafelski, J. Phys. G 28, 1911 (2002); C. Markert et al., arXiv:hep-ph/0206260v2 (2002)

Hadronization at intermediate momenta

- Baryon puzzle - increased B/M (p/π, Λ/K_s^0 , Λ_c^+/D etc.) ratios at RHIC and the LHC

- Driving force of enhancement is not yet fully understood:

✓ particle mass (hydro)?

✓ quark count (baryons vs. mesons)?

- ϕ and K^{*0} are well suited for tests as mesons with masses very close to that of a proton:

✓ $\Delta m_\phi \sim$ 80 MeV/c^2, $\Delta m_{K^{*0}} \sim$ -45 MeV/c^2

Phys.Lett. B736 (2014) 196-207

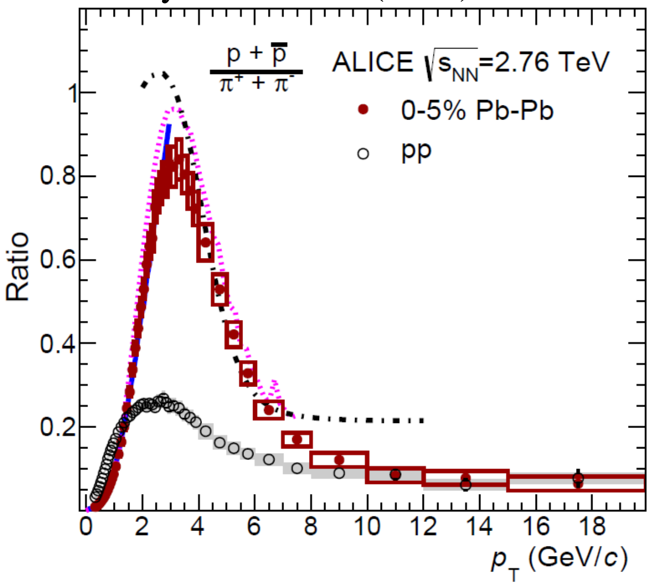

Phys.Rev. C88 (2013) 2, 024906

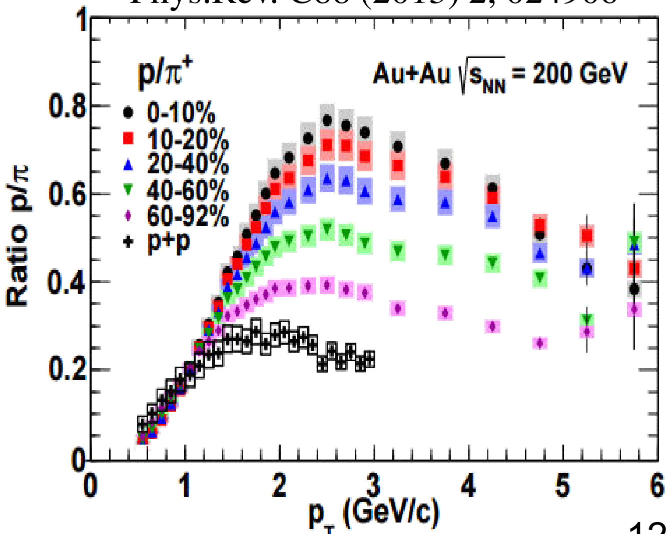

Particle ratios: $p/\phi(p_T)$, $p/K^*(p_T)$

- In peripheral p-Pb and Pb-Pb collisions ratios are similar to that in pp
- $p/\phi(p_T)$ and $p/K^*(p_T)$ evolve with centrality and flatten in most **central Pb-Pb** collisions
  - → similar spectral shapes of p, K^* and ϕ
  - → spectral shapes are determined by masses, consistent with hydrodynamic evolution
- p/ϕ in high-multiplicity p-Pb indicates flattering of the ratio at $p_T < 1.5$ GeV/*c*
  → hint of the onset of collective behaviour in p-Pb?
- RHIC results show similar flattening but within larger uncertainties

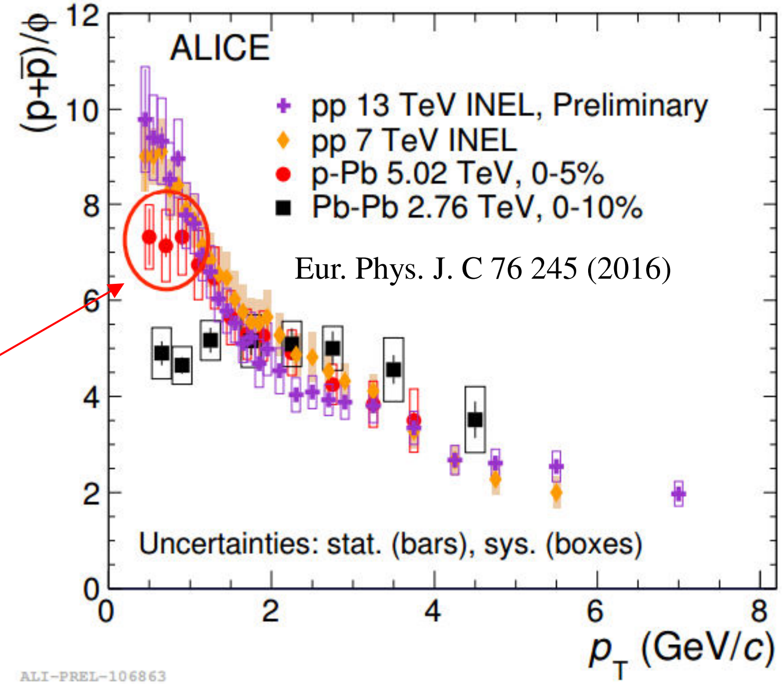

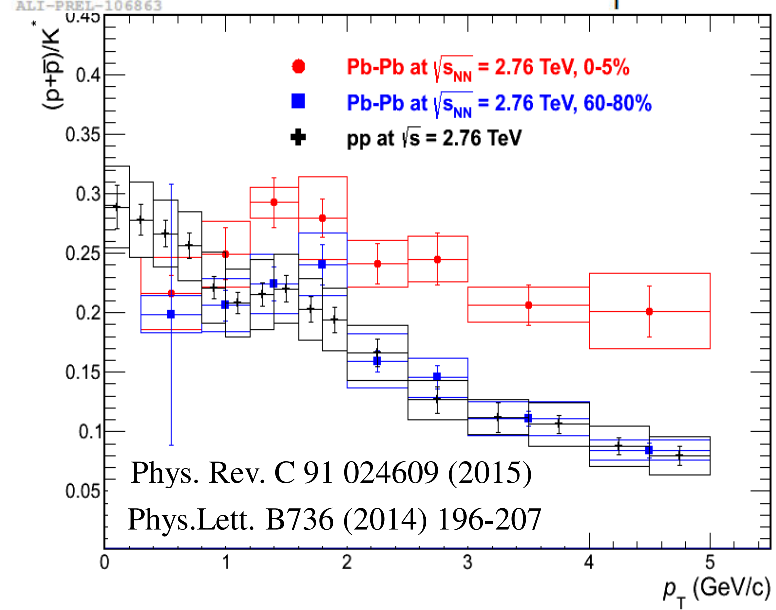

ALICE results in CERN Courier

ALICE sheds light on particle production in heavy-ion collisions

New results from the ALICE collaboration are providing additional data to test ideas about how particles are produced out of the quark–gluon plasma (QGP) created in heavy-ion collisions at the LHC.

Experiments at Brookhaven's Relativistic Heavy Ion Collider (RHIC) observed an enhancement in p_T-dependent baryon/meson ratios – specifically the p/π and Λ/K^0_S ratios – for central nucleus–nucleus (AA) collisions in comparison with proton–proton (pp) collisions, where particle production is assumed to be dominated by parton fragmentation. In addition, constituent-quark scaling was observed in the elliptic-flow parameter, v_2, measured in AA collisions. To interpret these observations, the coalescence of quarks was suggested as an additional particle-production mechanism. The coalescence (or recombination) model postulates that three quarks must come together to form a baryon, while a quark and an antiquark must coalesce to form a meson. The p_T and the v_2 of the particle created is the sum of the respective values of the constituent quarks. Therefore, coalescence models generally predict differences between the p_T spectra of baryons and mesons, predominantly in the range $2 < p_T < 5$ GeV/c, where the enhancement in the baryon/meson ratio has been measured.

While a similar enhancement in the p/π and Λ/K^0_S ratios is observed at the LHC, the mass scaling of v_2 is not, calling into question the importance of the coalescence mechanism. The observed-particle p_T spectra reflect the dynamics of the expanding QGP created in local thermal equilibrium, conferring to the final-state particles a common radial velocity independent of their mass, but a different momentum (hydrodynamic flow). The resulting blue shift in the p_T spectrum therefore scales with particle mass, and is observed as a rise in the p/π and Λ/K^0_S ratios at low p_T (see figure). In such a hydrodynamic description, particles with the same mass have p_T spectra with similar shapes, independent of their quark content. The particular shape of the baryon/meson ratio observed in AA collisions therefore reflects the relative importance of hydrodynamic flow, parton fragmentation and quark coalescence. However, for the p/π and Λ/K^0_S ratios, the particles in the numerator and denominator differ in both mass and (anti)quark content, so coalescence and hydrodynamic effects cannot be disentangled. To test the role of coalescence further, it is instructive to conduct this study using a baryon and a meson that have similar mass.

Fortunately, nature provides two such particles: the proton, a baryon with mass 938 MeV/c^2, and the φ meson, which has a mass of 1019 MeV/c^2. If protons and φ mesons are produced predominantly through coalescence, their p_T spectra will have different shapes. Hydrodynamic models alone would predict p_T spectra with similar shapes owing to the small mass-difference (less than 9%), implying a p/φ ratio that is constant with p_T.

For peripheral lead–lead collisions, where the small volume of the quark–gluon plasma reduces the influence of collective hydrodynamic motion on the p_T spectra, the p/φ ratio has a strong dependence on p_T, similar to that observed for pp collisions.

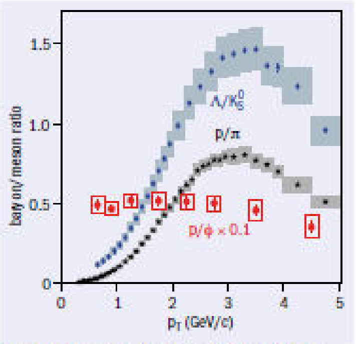

The flat dependence on p_T of the p/φ ratio measured by ALICE for central lead–lead collisions, compared with the p/π and Λ/K^0_S ratios, indicates hydrodynamics as the leading contribution to the p_T spectra.

In contrast, as the figure shows, in central lead–lead collisions – where the volume of the QGP produced is largest – the p/φ ratio has a very different p_T dependence, and is constant within its uncertainties for $p_T < 4$ GeV/c. The data therefore indicate that hydrodynamics is the leading contribution to particle p_T spectra in central lead–lead collisions at LHC energies, and it does not seem necessary to invoke coalescence models.

In the coming year, the ALICE collaboration will measure a larger number of collisions at a higher energy. This will allow a more precise study of both the p_T spectra and elliptic-flow parameters of the proton and φ meson, and will allow tighter constraints to be placed on theoretical models of particle production in heavy-ion collisions.

Further reading

B Abelev *et al.* ALICE Collaboration 2014 arXiv:1404.0495 [nucl-ex], accepted for publication in *Phys. Rev. C*.

Enhanced strangeness production

Nature Phys. 13 (2017) 535

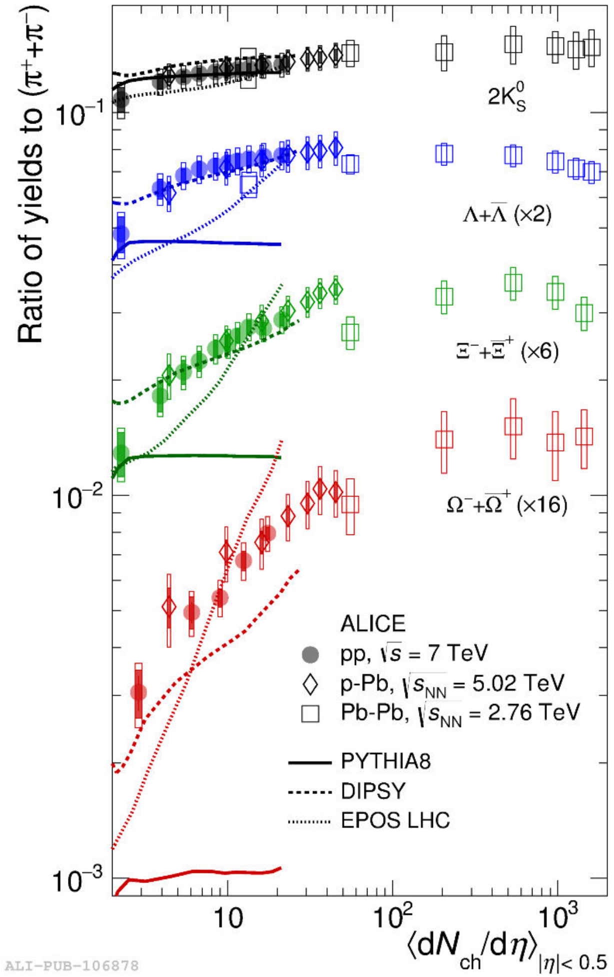

EPJ C77 (2017) 389

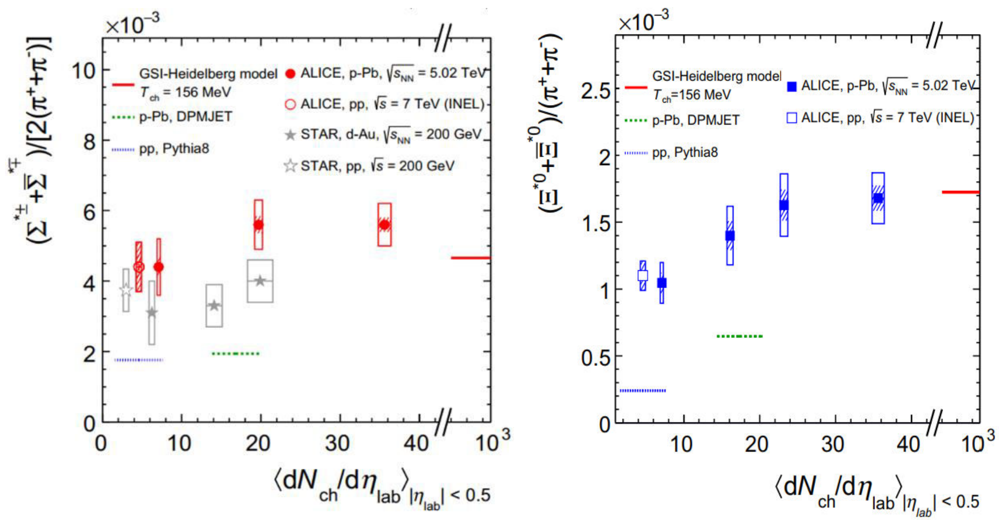

- Clear increase of strangeness production from pp to Pb-Pb
- First observation of enhanced production of strange particles in high-multiplicity pp collisions
- Strange resonances show increasing patterns depending on the strangeness content → consistent with observations for ground-state hadrons
- Thermal model predictions for Pb-Pb are consistent with the highest multiplicity results in p-Pb while PYTHIA and DPMJET underestimate data

Enhanced strangeness production, resonances

EPJ C77 (2017) 389

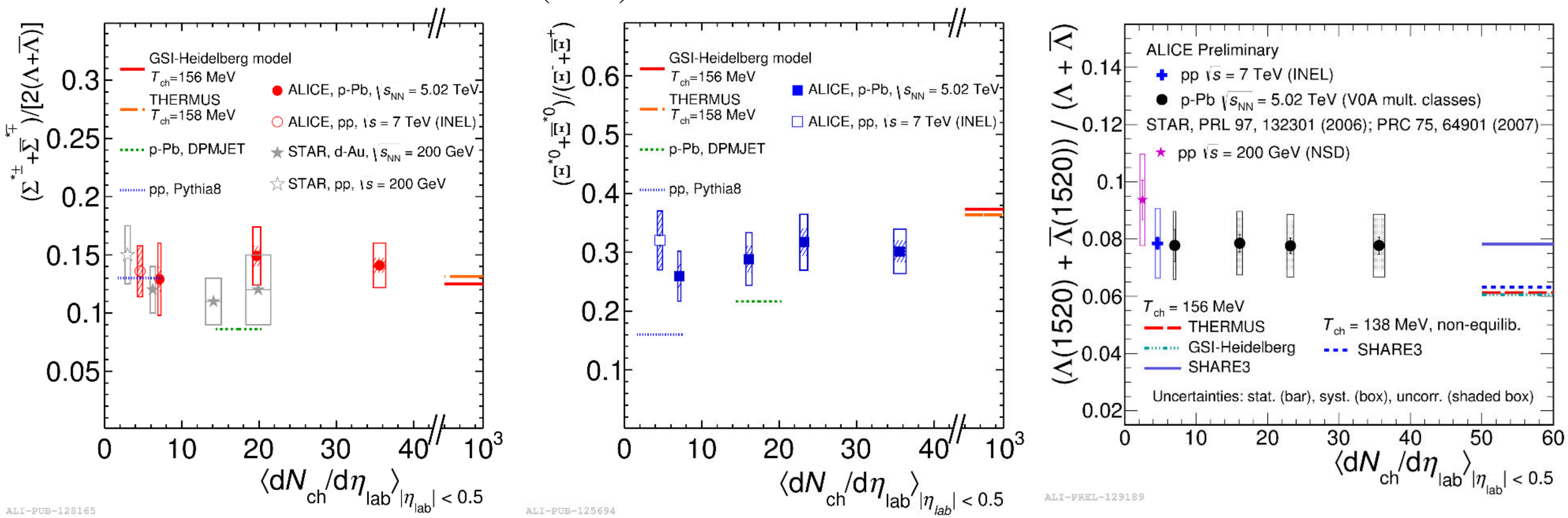

- Ratios of resonances to stable particles with the same strangeness do not depend on multiplicity in pp and p-Pb → confirms that strangeness enhancement depends predominantly on the strangeness content, rather than on the particle mass
- Ratios do not show strong dependence on collision energy, √s = 0.2–5.02 TeV
- No model reproduces all measurements simultaneously

Enhanced strangeness production, ϕ is a key!

- The ϕ meson (s-sbar) has hidden strangeness and is a key probe in studying strangeness production
- Particles with open strangeness are subject to canonical suppression in small systems (strangeness conservation in strong interactions), while ϕ is not
- Experiment:
  - ✓ small systems - ϕ/π increases with multiplicity → not expected for canonical suppression
  - ✓ large systems → ϕ production is consistent with thermal models
- Ratios ϕ/K and Ξ/ϕ are flat across wide multiplicity range → ϕ has "effective" strangeness of 1-2

ϕ/π: (|S|=0)/(|S|=0)

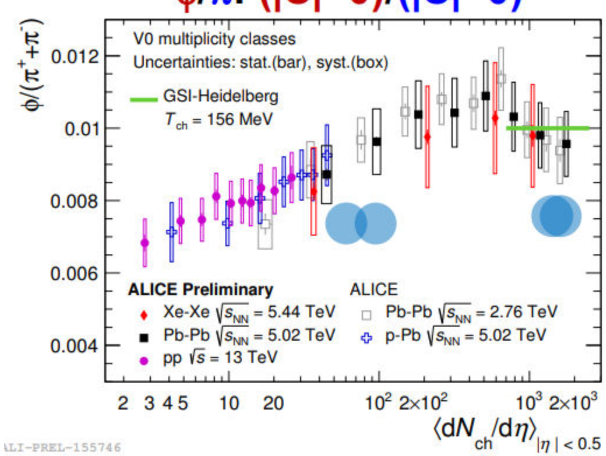

ϕ/K: (|S|=0)/(|S|=1)

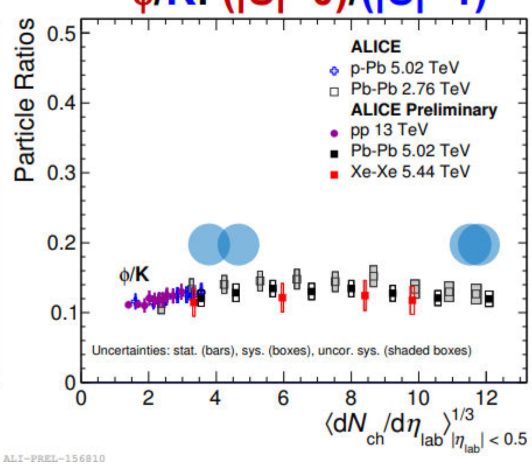

Ξ/ϕ: (|S|=2)/(|S|=0)

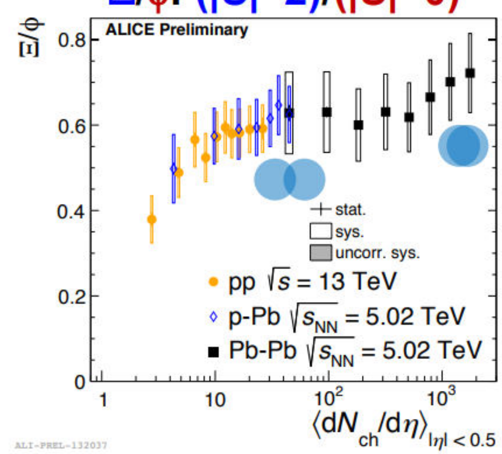

Many more reasons to study resonances …

- jet quenching vs. parton flavor/mass
- flow build-up
- background signals for other analyses
- cross check with e^+e^- measurements
- etc.

What unites all resonances …

- similar analysis approaches (FG, BG, peak models, fit procedures)
- probes of the same physics phenomena

Reconstruction of resonances

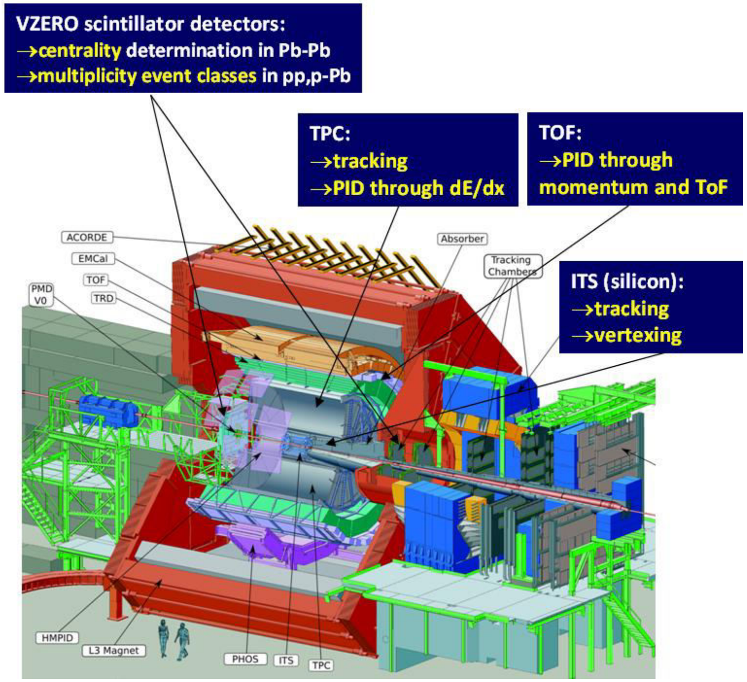

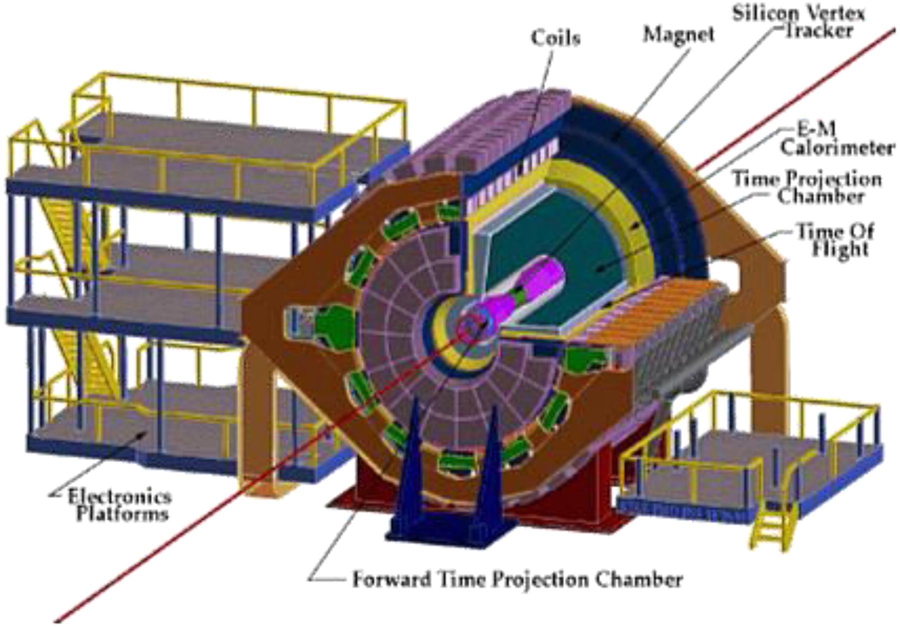

- The main resonance measurements were produced by STAR and ALICE
- Both experiments have detector layouts similar to that of the MPD:
  - ✓ TPC (and ITS): tracking + PID
  - ✓ TOF: PID
- Feasibility of the resonance measurements in the MPD depends on production cross sections, background levels and detector performance

Expectations for resonances at NICA

- Resonance yields and combinatorial background can be estimated using different event generators, tuned based on expected particle ratios and scalings
- Selection of the event generator is not trivial:
    - ✓ should know resonances
    - ✓ realistic yields vs. p_T and rapidity for resonances
    - ✓ realistic yields for background, mostly charged hadrons
    - ✓ chiral symmetry restoration effects for resonances (unlikely)
    - ✓ hadronic cascade

… work in progress

Current approach

- Simulated minbias AuAu@11 collisions using UrQMD 3.4 with default settings
- UrQMD as a hadronic cascade afterburner to EPOS3 was extremely successful in description of the resonance properties in AA collisions at RHIC and the LHC
- UrQMD let us follow the resonances and their decay products using *f14* (final state particles) and *f15* (processes) output files

Examples of processes for ρ (PID = 104)

- 2 → 7, BB → 2 strings, direct production of ρ:

2 7 15 21 0.827 0.6823E+01 0.4000E+02 0.2419E+02 0.1081E+01

132	0.82684166E+00	-0.22080446E+00	-0.40028488E+00	-0.36857956E+00	0.37502111E+01	-0.25938156E+00	0.84495105E+00	0.35217918E+01	0.93800002E+00	1	-1	0	17	2	0	200
438	0.82684166E+00	0.61169107E-01	-0.13753055E+00	-0.36944866E+00	0.32676586E+01	-0.10745271E+00	0.58955632E+00	-0.28107900E+01	0.15549692E+01	20	1	1	15	1	0	17001035
456	0.82684166E+00	-0.22080446E+00	-0.40028488E+00	-0.36857956E+00	0.21104126E+01	0.45995911E+00	0.66541395E+00	0.17087010E+01	0.93800002E+00	1	1	1	21	3	0	20001015
457	0.82684166E+00	0.61169107E-01	-0.13753055E+00	-0.36944866E+00	0.14786775E+01	-0.38783507E-01	-0.18018397E+00	-0.11281280E+01	0.93800002E+00	1	-1	0	21	2	0	20001015
458	0.82684166E+00	-0.22080446E+00	-0.40028488E+00	-0.36857956E+00	0.12573262E+01	-0.45415420E+00	-0.10531048E+00	0.94633326E+00	0.68408794E+00	104	0	0	21	1	0	20001015
459	0.82684166E+00	-0.22080446E+00	-0.40028488E+00	-0.36857956E+00	0.63126889E+00	-0.29771500E-01	0.27538770E+00	0.38913863E-01	0.56591642E+00	104	0	0	21	1	0	20001015
460	0.82684166E+00	-0.22080446E+00	-0.40028488E+00	-0.36857956E+00	0.25907173E+00	-0.13433291E+00	0.14677015E+00	0.92126841E-01	0.13800000E+00	101	-2	-1	21	1	0	20001015
461	0.82684166E+00	0.61169107E-01	-0.13753055E+00	-0.36944866E+00	0.90582489E+00	0.76201314E-01	0.51068425E+00	-0.73134786E+00	0.13800000E+00	101	0	0	21	1	0	20001015
462	0.82684166E+00	0.61169107E-01	-0.13753055E+00	-0.36944866E+00	0.37528775E+00	-0.24595258E+00	0.12174578E+00	-0.21559728E+00	0.13800000E+00	101	2	1	21	1	0	20001015

- 2 → 2, MM elastic scattering, this time ρK→ρK

2 2 38 221 4.419 0.1389E+01 0.8795E+01 0.5000E+01 0.1372E+00

497	0.44186141E+01	-0.16379463E+01	-0.70785629E+00	0.24273881E+01	0.13214302E+01	-0.59629122E+00	0.59263440E+00	0.89183125E+00	0.49399999E+00	106	1	1	35	1	-1	1001015
458	0.44186141E+01	-0.15181754E+01	-0.70112269E+00	0.23347870E+01	0.12573262E+01	-0.45415420E+00	-0.10531048E+00	0.94633326E+00	0.68408794E+00	104	0	0	21	1	0	20001015
497	0.44186141E+01	-0.16379463E+01	-0.70785629E+00	0.24273881E+01	0.12864324E+01	-0.81118491E+00	0.38601475E-01	0.86681104E+00	0.49399999E+00	106	1	1	221	2	-1	1001115
458	0.44186141E+01	-0.15181754E+01	-0.70112269E+00	0.23347870E+01	0.12923240E+01	-0.23926051E+00	0.44872245E+00	0.97135347E+00	0.68408794E+00	104	0	0	221	2	0	20001115

- 1 → 2, decay, this time ρ→ππ

1 2 20 247 4.958 0.6841E+00 0.0000E+00 0.0000E+00 0.1203E+00

458	0.49578933E+01	-0.16180174E+01	-0.51387344E+00	0.27401271E+01	0.12923240E+01	-0.23926051E+00	0.44872245E+00	0.97135347E+00	0.68408794E+00	104	0	0	221	2	0	20001115
892	0.49578933E+01	-0.16180174E+01	-0.51387344E+00	0.27401271E+01	0.75387218E+00	-0.20680107E+00	-0.11783587E-02	0.71169600E+00	0.13800000E+00	101	2	1	247	3	0	104020
893	0.49578933E+01	-0.16180174E+01	-0.51387344E+00	0.27401271E+01	0.53845181E+00	-0.32459439E-01	0.44990081E+00	0.25965747E+00	0.13800000E+00	101	-2	-1	247	1	0	104020

- 1 → 2, decay, this time Δ_{1950}→pρ, feed down production (from decays)

1 2 20 156 2.901 0.2750E+01 0.0000E+00 0.0000E+00 0.2348E+00

734	0.29006275E+01	-0.76626516E+00	0.34443468E+01	-0.67954851E+00	0.51184882E+01	-0.95182794E-01	0.14826380E+00	-0.43134112E+01	0.27499751E+01	26	1	1	140	3	0	1017035
757	0.29006275E+01	-0.76626516E+00	0.34443468E+01	-0.67954851E+00	0.20976020E+01	-0.48815429E-01	-0.93407670E+00	-0.16264095E+01	0.93800002E+00	1	1	1	156	4	0	26020
758	0.29006275E+01	-0.76626516E+00	0.34443468E+01	-0.67954851E+00	0.30208862E+01	-0.46367365E-01	0.10823405E+01	-0.26870017E+01	0.85566603E+00	104	0	0	156	1	0	26020

- 1 → 2, ρ→ππ decay + 2 →1 (πp → Δ_{1232}) recombination → daughter pion lost

1 2 20 142 6.594 0.7906E+00 0.0000E+00 0.0000E+00 0.5329E-01

653	0.65943555E+01	0.17904484E+01	0.28368141E+01	0.37521573E+01	0.10146263E+01	0.20236244E+00	-0.68622156E-01	0.59890372E+00	0.79064619E+00	104	0	0	134	1	0	114020
663	0.65943555E+01	0.17904484E+01	0.28368141E+01	0.37521573E+01	0.37933209E+00	0.35324475E+00	-0.81712575E-02	0.45990110E-03	0.13800000E+00	101	-2	-1	142	2	0	104020
664	0.65943555E+01	0.17904484E+01	0.28368141E+01	0.37521573E+01	0.63529426E+00	-0.15088231E+00	-0.60450898E-01	0.59844382E+00	0.13800000E+00	101	2	1	142	1	0	104020

2 1 10 163 7.770 0.1203E+01 0.1635E+03 0.1635E+03 0.8367E-01

664	0.77700297E+01	0.15112259E+01	0.27249438E+01	0.48596362E+01	0.63529426E+00	-0.15088231E+00	-0.60450898E-01	0.59844382E+00	0.13800000E+00	101	2	1	142	1	0	104020
627	0.77700297E+01	0.17760407E+01	0.20872806E+01	0.51750898E+01	0.34495267E+01	0.31485445E+00	0.16791848E+00	0.33003122E+01	0.93800002E+00	1	1	1	117	2	0	22020
697	0.77700297E+01	0.16436333E+01	0.24061122E+01	0.50173630E+01	0.40848210E+01	0.16397214E+00	0.10746758E+00	0.38987560E+01	0.12029247E+01	17	3	2	163	3	0	1101010

Hadronic phase effects, framework

- Estimate hadronic phase effects for the short and long lived resonances - ρ and ϕ
- Accumulated p_T distributions of ρ and ϕ mesons taking into account the following processes:
  - ✓ (1) – direct production + from decays + scattering (no loss of daughter + 3σ mass cut = still reconstructable) + recombination
  - ✓ (2) – direct production + from decays + scattering (no loss of daughter) + scattering (loss of daughter)

- Spectrum (2) approximates directly produced particles
- Spectrum (1) approximates directly produced particles + hadronic phase effects
- Ratio (1)/(2) shows how hadronic phase affects the particle spectra and yields

Hadronic phase effects, yields of ρ

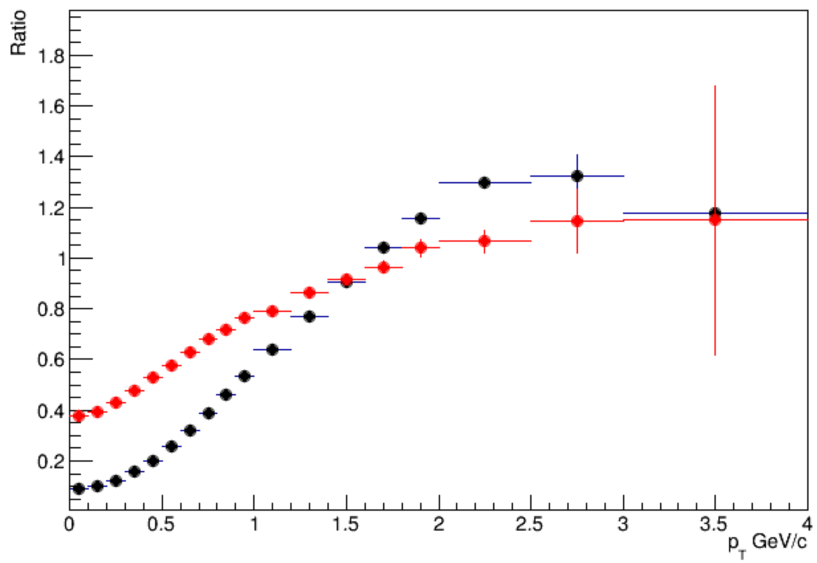

- **Central collisions (0-5 fm)**:
  - ✓ very strong suppression of the ρ yields at low momentum due to loss of daughters
  - ✓ enhanced ρ production at intermediate momenta due to hadron recombination
  - ✓ ratio returns to unity at higher momenta
- **Non-central collisions (10-15 fm)**:
  - ✓ contribution of rescattering with loss of daughter pions is still significant
  - ✓ regeneration does not result in enhancement at intermediate momenta

Hadronic phase effects, mass of ρ

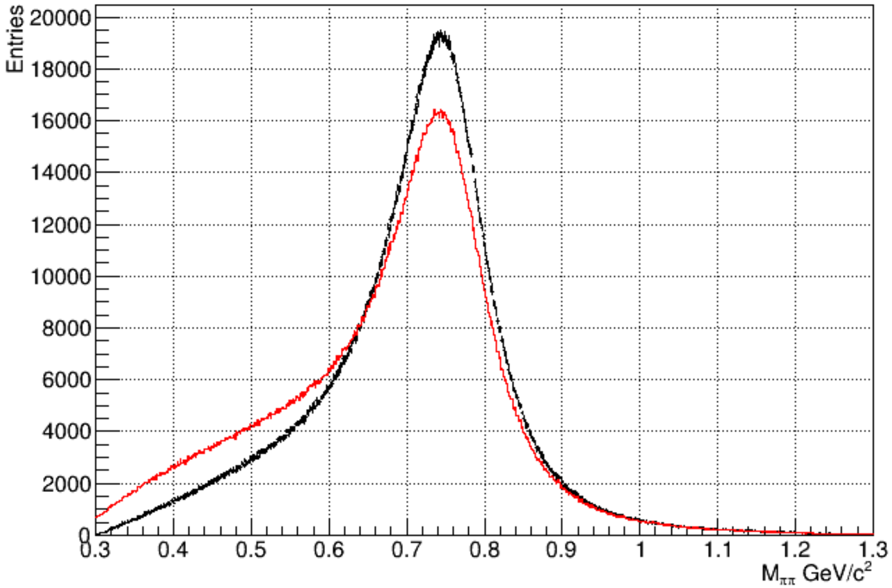

- **Reconstructed masses** differ from the **generated ones** due to rescattering of the daughter pions (broken angular correlations, momentum changes) and pion recombination (favors lower masses due to steep p_T spectrum of pions)

Hadronic phase effects, yields of ϕ

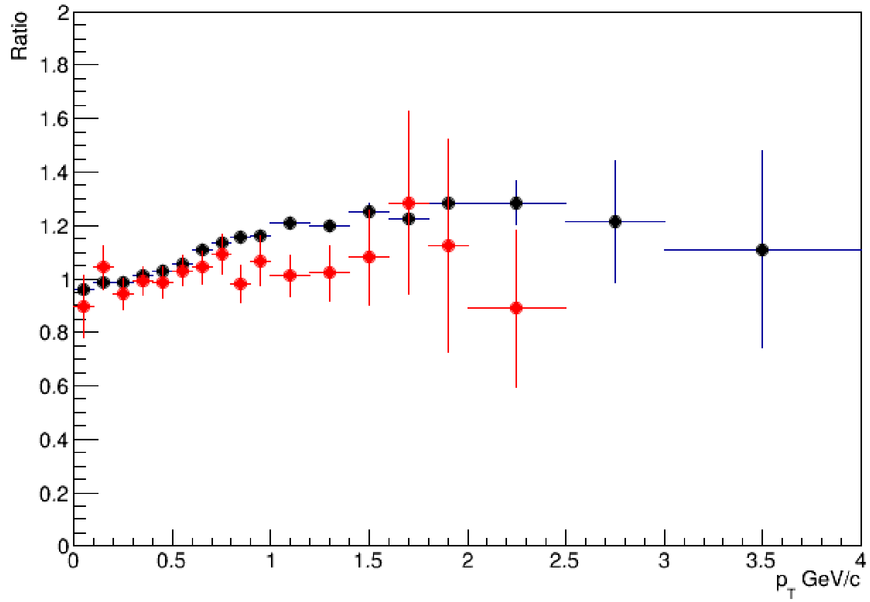

- **Central collisions (0-5 fm)**:
  - ✓ very weak suppression of the ϕ yields at low momentum
  - ✓ enhanced ϕ production at intermediate momenta due to hadron recombination
  - ✓ ratio returns to unity at higher momenta
- **Non-central collisions (10-15 fm)**:
  - ✓ no effects within uncertainties

Hadronic phase effects, mass of ϕ

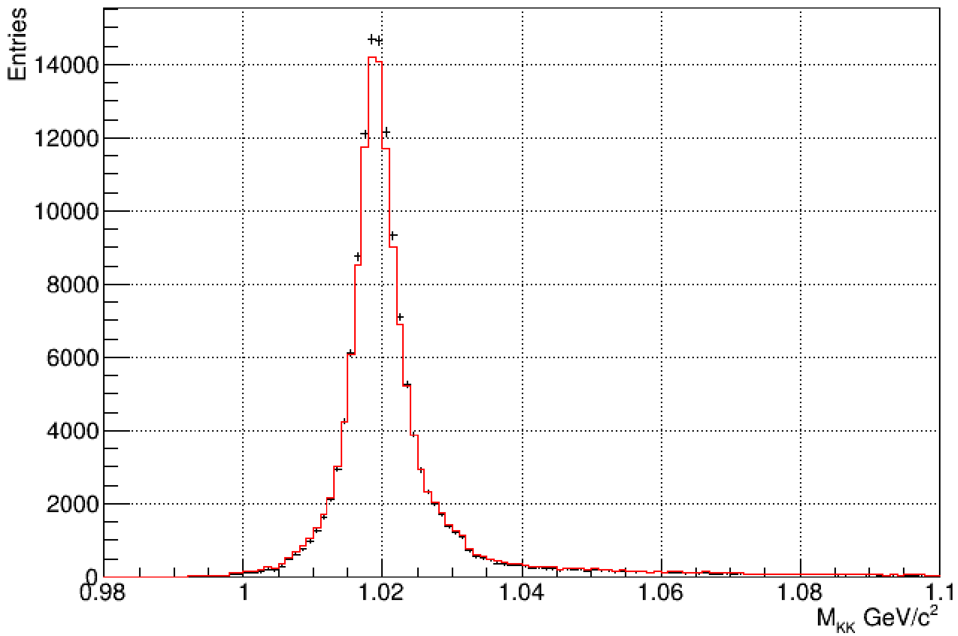

- **Reconstructed masses** are similar to **generated ones**

Hadronic phase effects, comparison to ALICE

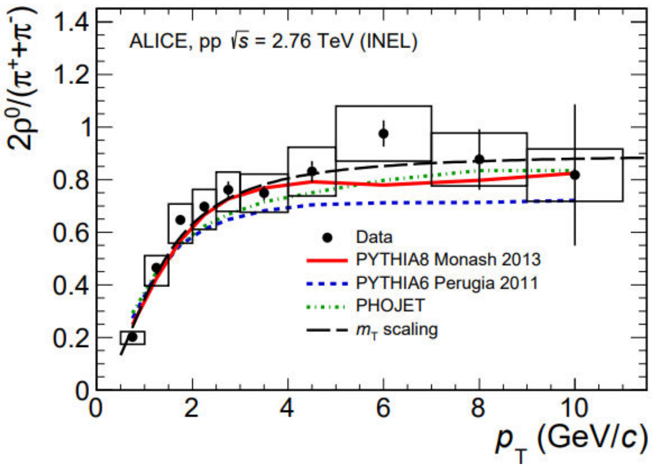

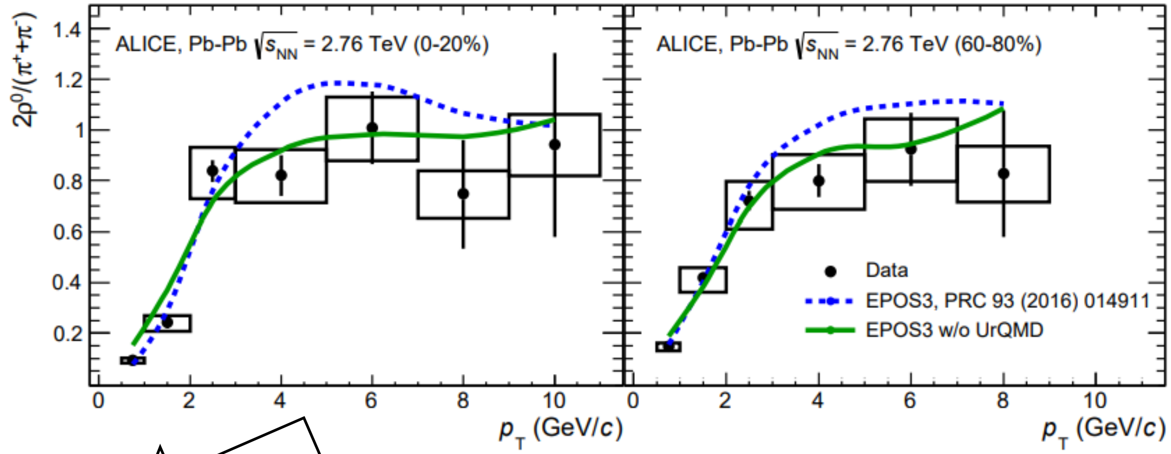

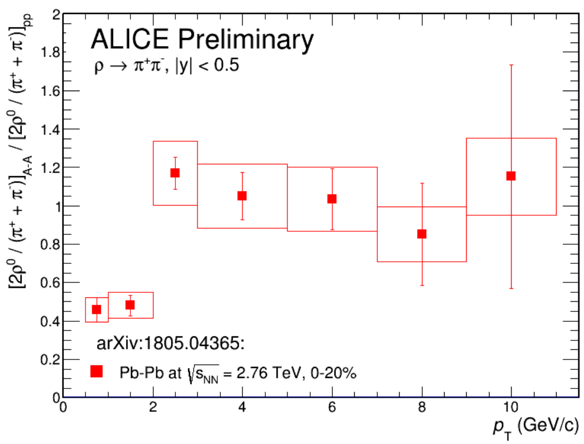

≈

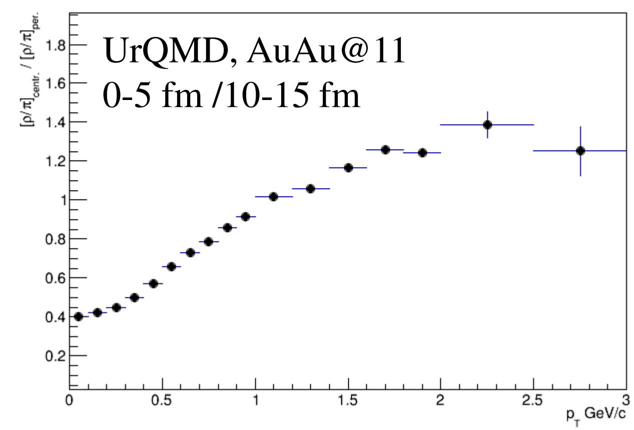

- Very similar suppression pattern measured by ALICE at the LHC
- Similar peak shape modifications are favored by data at the LHC

Feasibility studies for resonances, framework

- Simulated minbias AuAu@11 collisions using UrQMD 3.4 with default settings:
  - ✓ declare resonances as stable particles (no decays, no hadronic phase)
- Traced the particles through the MPD using ‘mpdroot’:
  - ✓ introduced resonances to Geant3 according to the PDG
  - ✓ handled resonance decays and propagation using Geant3 (no matter effects)
- DCA corrections after reconstruction using ‘restore_dca.c’
- DCA(x,y,z) parameterization vs. p_T and rapidity using the code developed by the Flow (MEPhI) group
- Combined TPC-TOF haron PID using ‘mpdpid class’ by A. Mudrokh

Analysis cuts & methods

- Event selection:
  - ✓ 0.5 M events
  - ✓ no centrality selections → minbias AuAu@11 by UrQMD3.4
  - ✓ $|Z_{vrtx}| < 50$ cm
- Track selection:
  - ✓ number of TPC hits > 39
  - ✓ $|\eta| < 1.0$
  - ✓ $|DCA(x,y,z)| < 2\sigma$
  - ✓ $p_T > 50$ MeV/c
  - ✓ TPC-TPF PID probability (π/K/p) > 0.75
  - ✓ TPC sector edges cut
- Pair cuts:
  - ✓ $|y| < 1.0$
- Combinatorial background:
  - ✓ event mixing ($|\Delta_{Zvrtx}| < 2$ cm, $|\Delta_{Mult}| < 20$, $N_{ev} = 10$) → worse description, smaller stat. unc.
  - ✓ like-sign background → better description, larger stat. unc. → kept for later

Feasibility study, ϕ

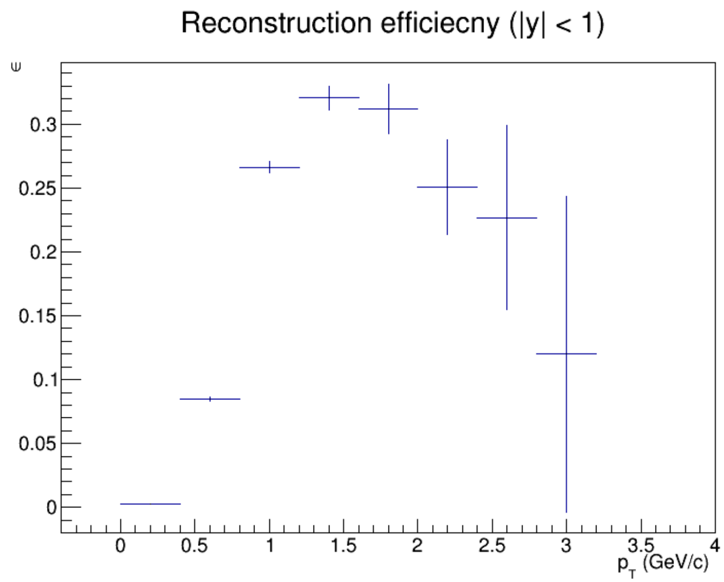

- Acceptance x reconstruction efficiency:

  $\in = N_{rec}(\phi \rightarrow KK, |y|<1) / N_{gen}(\phi \rightarrow KK, |y|<1)$

- Signal is seen, mass resolution is comparable to the natural width of ϕ ($\Gamma \sim 4$ MeV/c^2) → nearly Gaussian peak shape

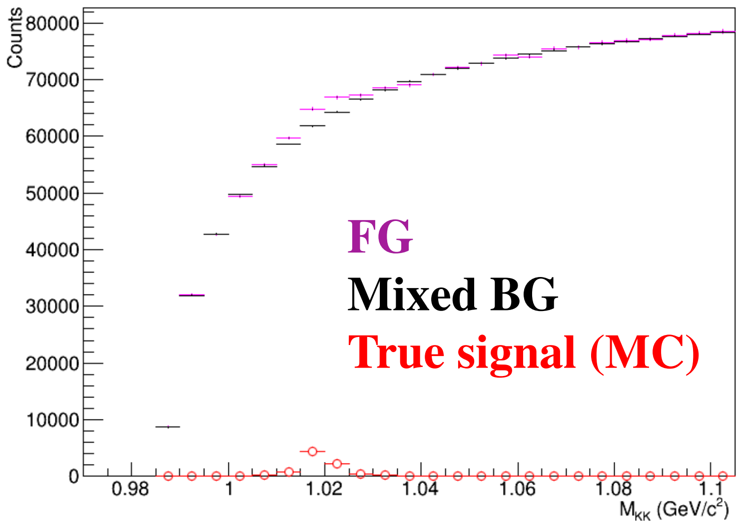

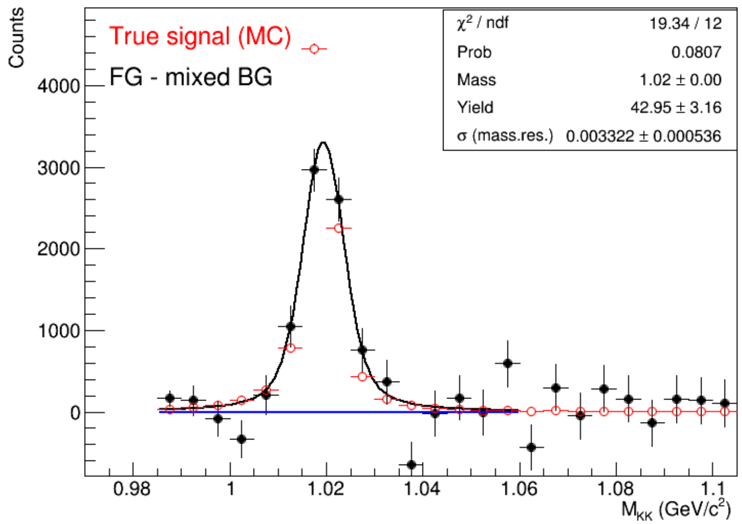

Feasibility study, ϕ

$0 < p_T$ (GeV/c) < 0.5

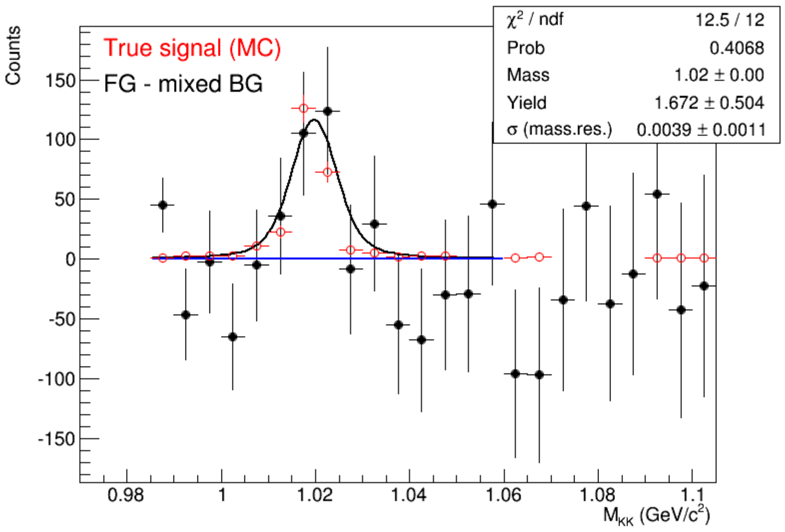

$1 < p_T$ (GeV/c) < 2

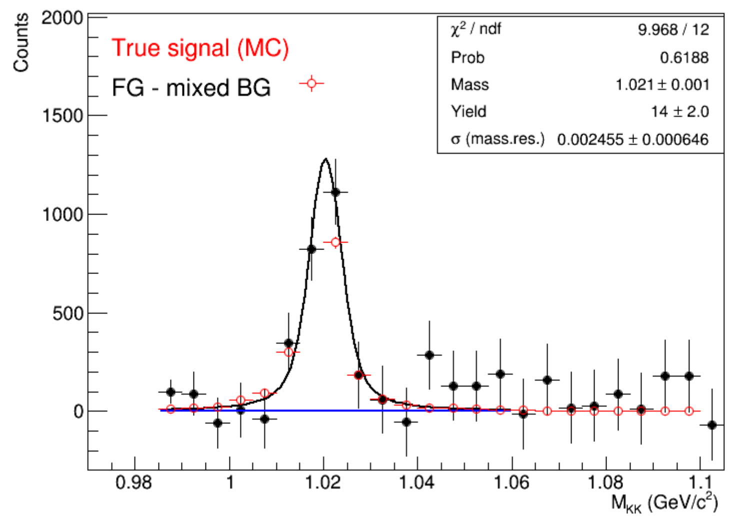

- Signal is seen at ~ zero momentum → integrated yields, $\langle p_T \rangle$ & low-p_T phenomena
- High-p_T reach of the measurements is limited by available statistics

Feasibility study, K^{*0}

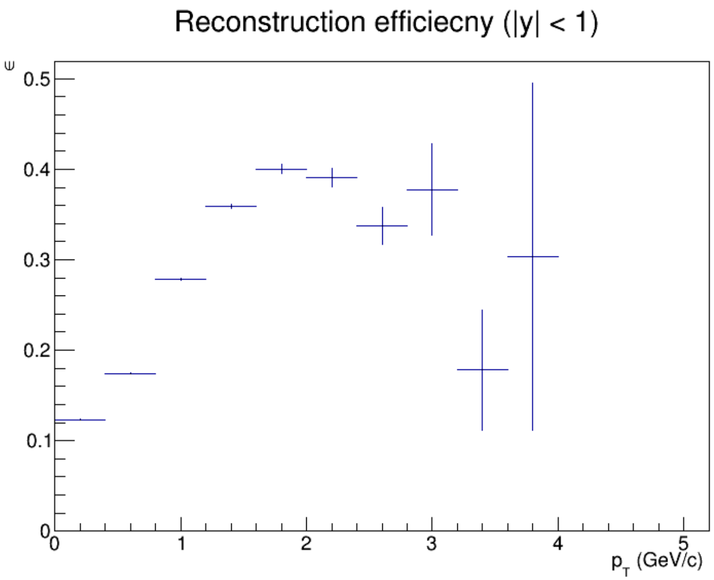

Acceptance x reconstruction efficiency:

$\in = N_{rec}(K^* \rightarrow K\pi, |y|<1) \, / \, N_{gen}(K^* \rightarrow K\pi, |y|<1)$

- Signal is seen, mass resolution << natural width of ϕ (Γ ~ 50 MeV/c^2) → (r)BW peak shape

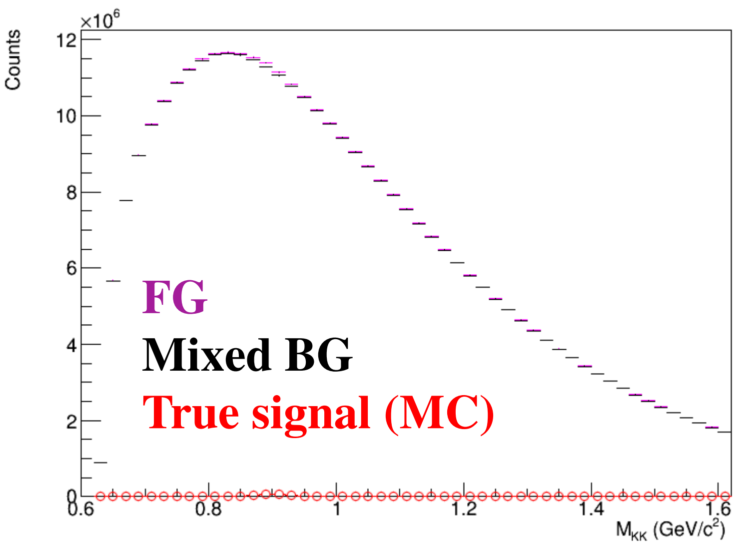

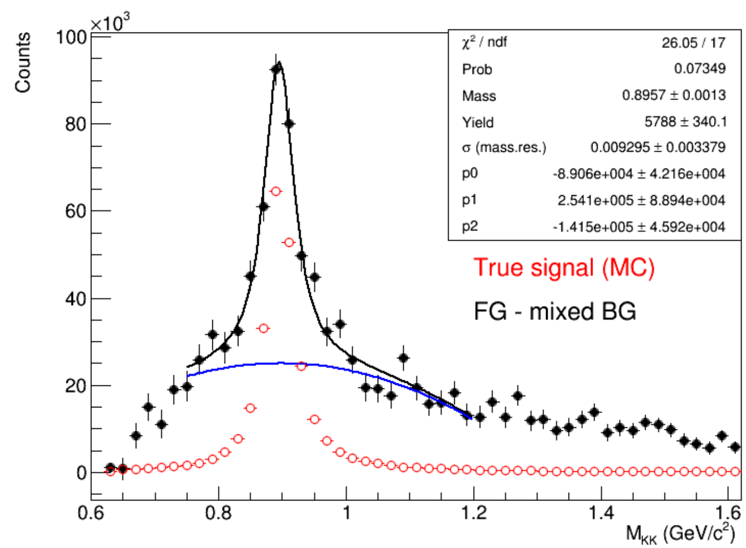

Feasibility study, K^{*0}

$0 < p_T$ (GeV/c) < 0.5

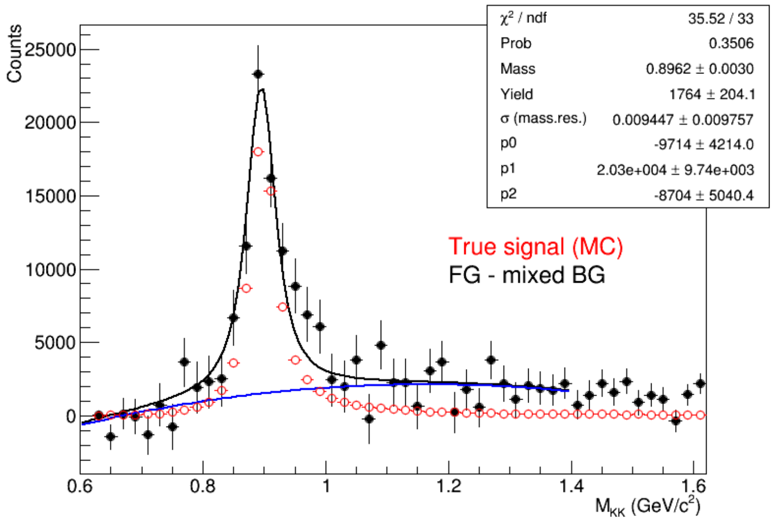

$1 < p_T$ (GeV/c) < 2

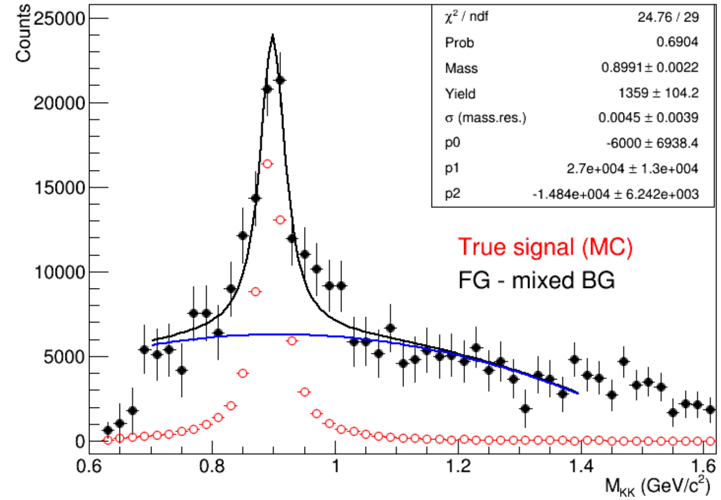

- Signal is seen at ~ zero momentum → integrated yields, $\langle p_T \rangle$ & low-p_T phenomena
- High-p_T reach of the measurements is limited by available statistics
- Peak shape is weakly affected by detector mass resolution

Feasibility study, ρ^0

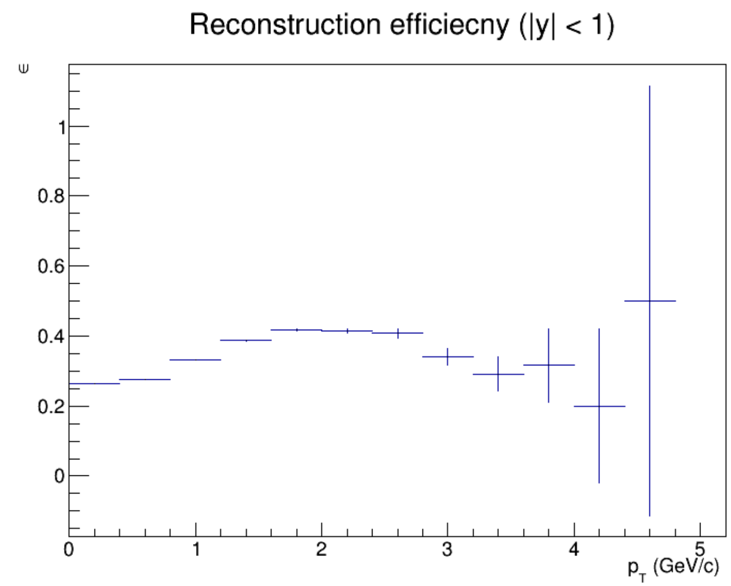

Acceptance x reconstruction efficiency:

$\epsilon = N_{rec}(\rho^0 \rightarrow \pi\ \pi, |y|<1) / N_{gen}(\rho^0 \rightarrow \pi\ \pi, |y|<1)$

- Signal is seen, mass resolution << natural width of ϕ (Γ ~ 150 MeV/c^2) → (r)BW peak shape

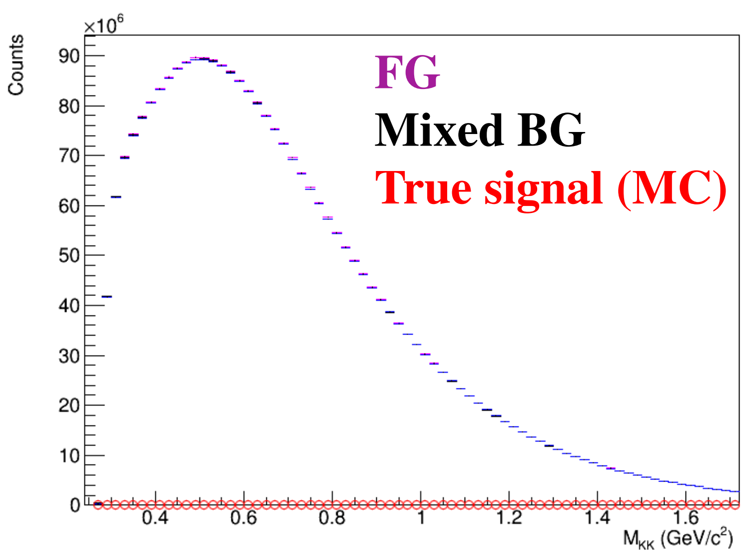

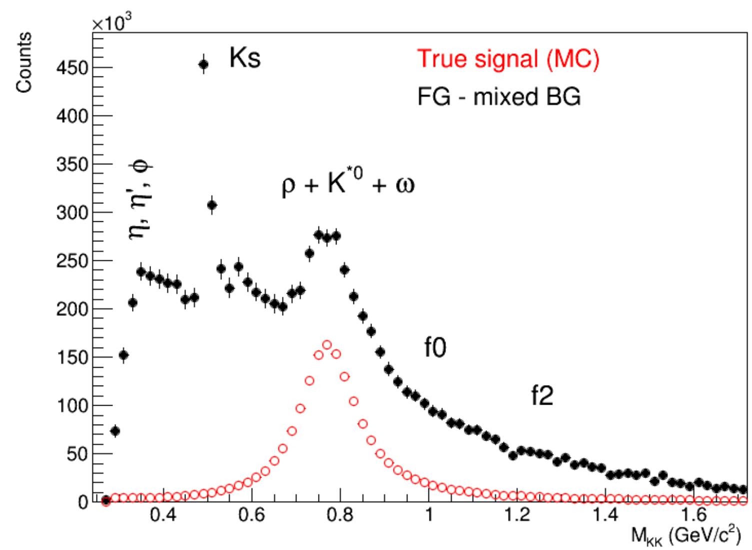

Feasibility study, ρ^0

arXiv:1805.04365, submitted to PRC

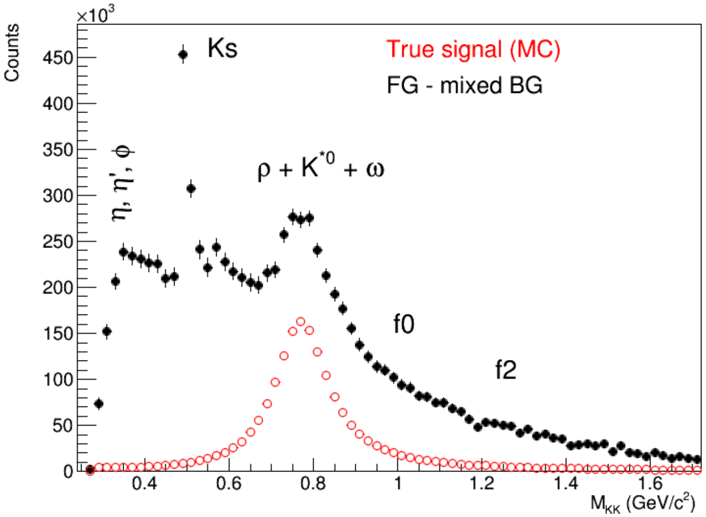

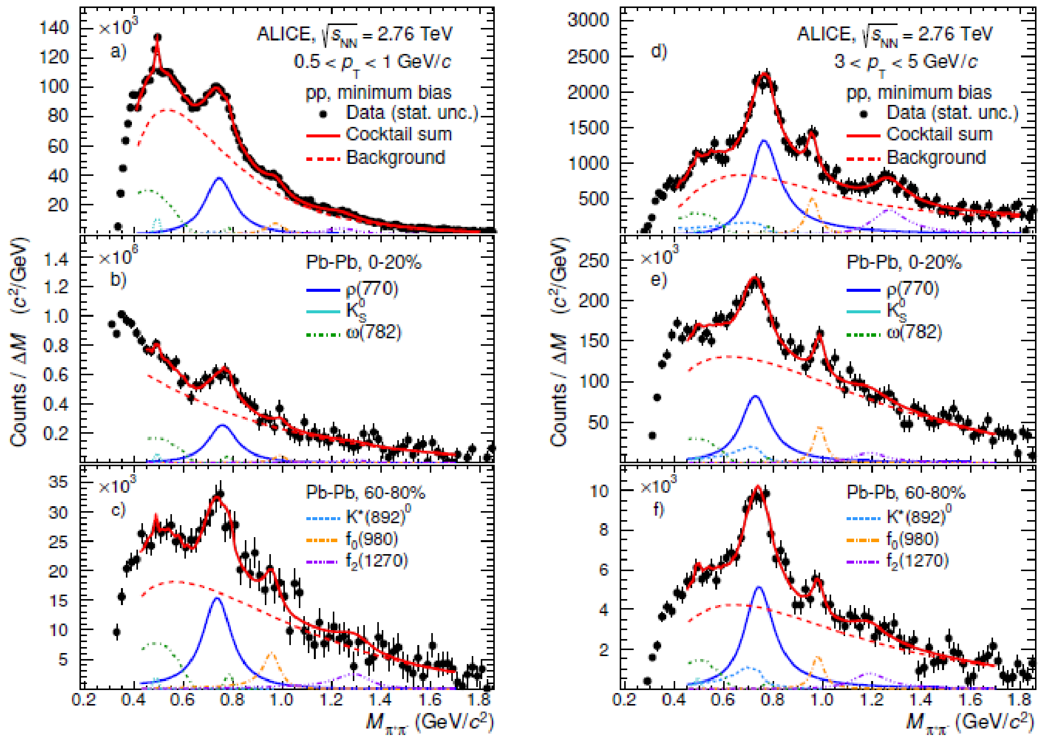

- Signal is seen
- Need to know yields of K^{*0}, ω, K → measurable
- Extracted yields are peak model dependent

Fig. 1: (Color online) Invariant mass distributions for $\pi^+\pi^-$ pairs after subtraction of the like-sign background. Plots on the left and right are for the low and high transverse momentum intervals, respectively. Examples are shown for minimum bias pp, 0–20% and 60–80% central Pb–Pb collisions at $\sqrt{s_{NN}} = 2.76$ TeV. Solid red curves represent fits to the function described in the text. Colored dashed curves represent different components of the fit function, which includes a smooth remaining background as well as contributions from K^0_S, ρ^0, $\omega(782)$, $K^*(892)^0$, $f_0(980)$ and $f_2(1270)$. See text for details.

Feasibility study, Λ(1520)

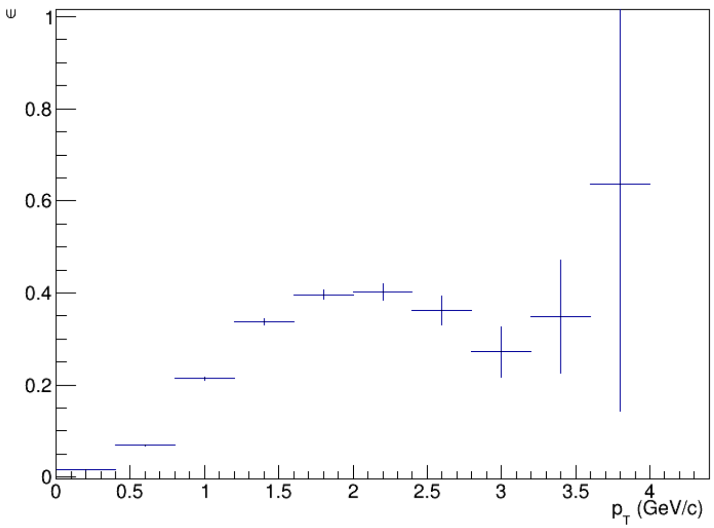

Acceptance x reconstruction efficiency:

$\in = N_{rec}(\Lambda^* \rightarrow pK, |y|<1) / N_{gen}(\Lambda^* \rightarrow pK, |y|<1)$

- Signal is seen, mass resolution < natural width of ϕ (Γ ~ 15 MeV/c^2) → modified (r)BW peak shape

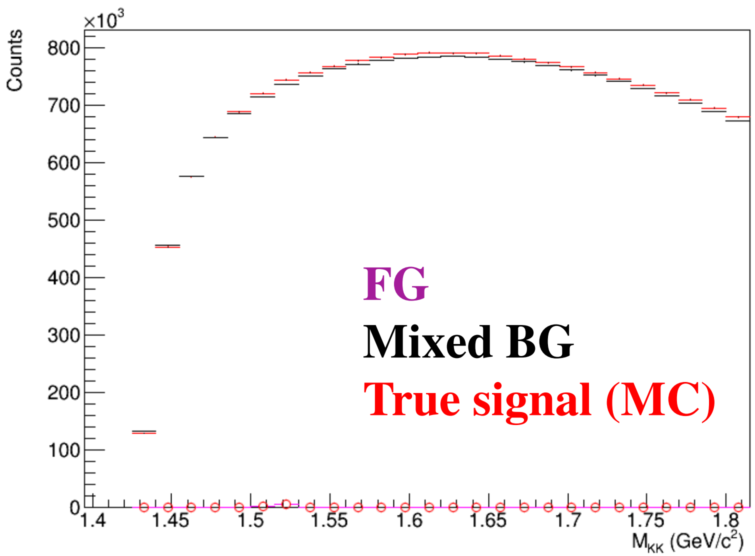

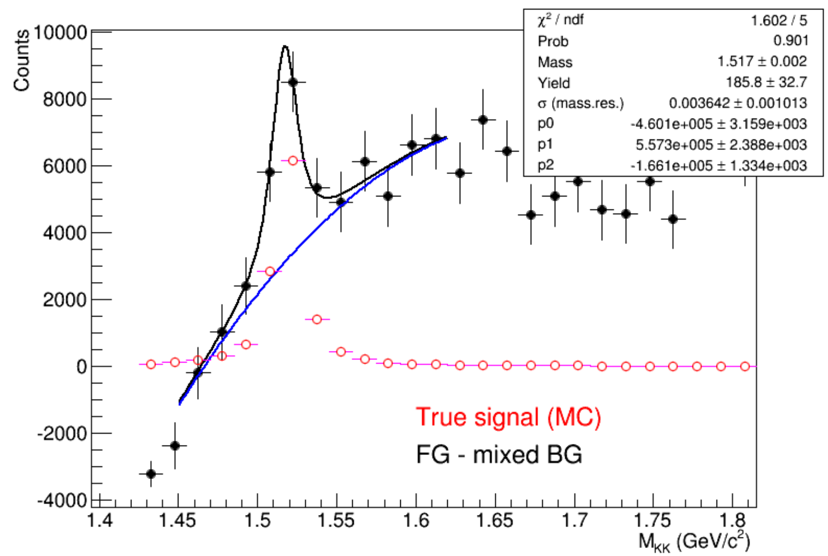

Summary

- ✓ Study of resonances is an important part of physical programs of the heavy-ion experiments at SPS-RHIC-LHC
- ✓ Resonances are expected to be sensitive to properties of the partonic/hadronic medium produced in heavy-ion collisions at NICA energies
- ✓ Resonances can potentially be measured using the MPD setup, more studies are needed/ongoing

⇩

Resonances are an important part of the MPD experimental program

Backup slides

Hadronic phase

- Simple model:
  - ✓ all K^{*0} that decayed before kinetic freeze-out are lost due to rescattering
  - ✓ regeneration and time dilation are ignored
  - ✓ Yield(central Pb-Pb) = Yield(pp)·exp(-Δt/τ), τ = 4.16 fm/*c* → Δt = 2.25±0.75 fm/*c*
  - ✓ Lower limit for hadronic phase lifetime: **Δt > 1.5 fm/*c***

- More advanced models [1,2] couple particle ratios to temperature and hadronic phase lifetime Δt:
  - ✓ T = 156 MeV from thermal fits
  - ✓ K^{*0}/K= 0.2 ±0.01 (stat) ± 0.03 (syst)

  → **Δt > 2 fm/*c***

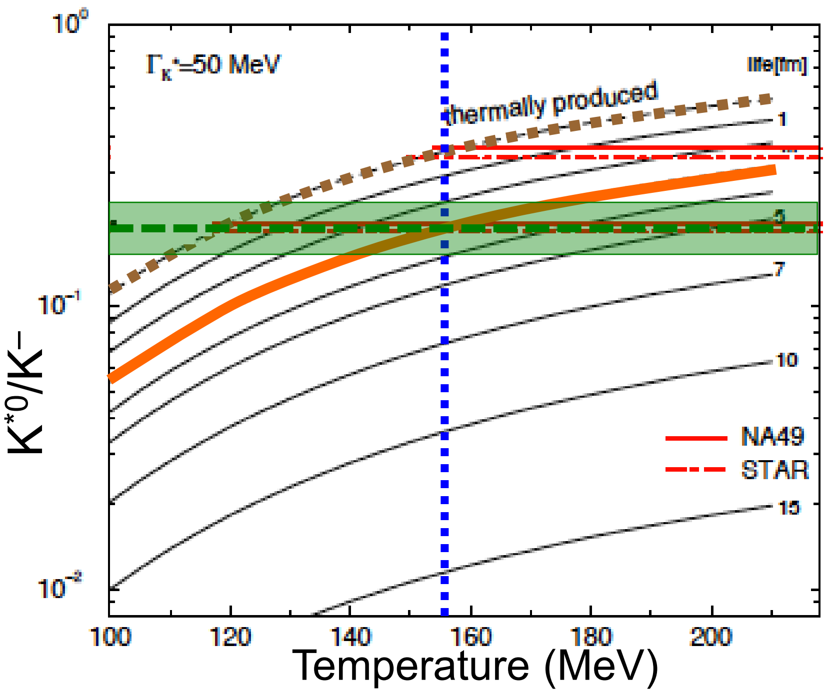

[1] G. Torrieri and J. Rafelski, J. Phys. G 28, 1911 (2002)

[2] C. Markert et al., arXiv:hep-ph/0206260v2 (2002)

EPOS3 + UrQMD

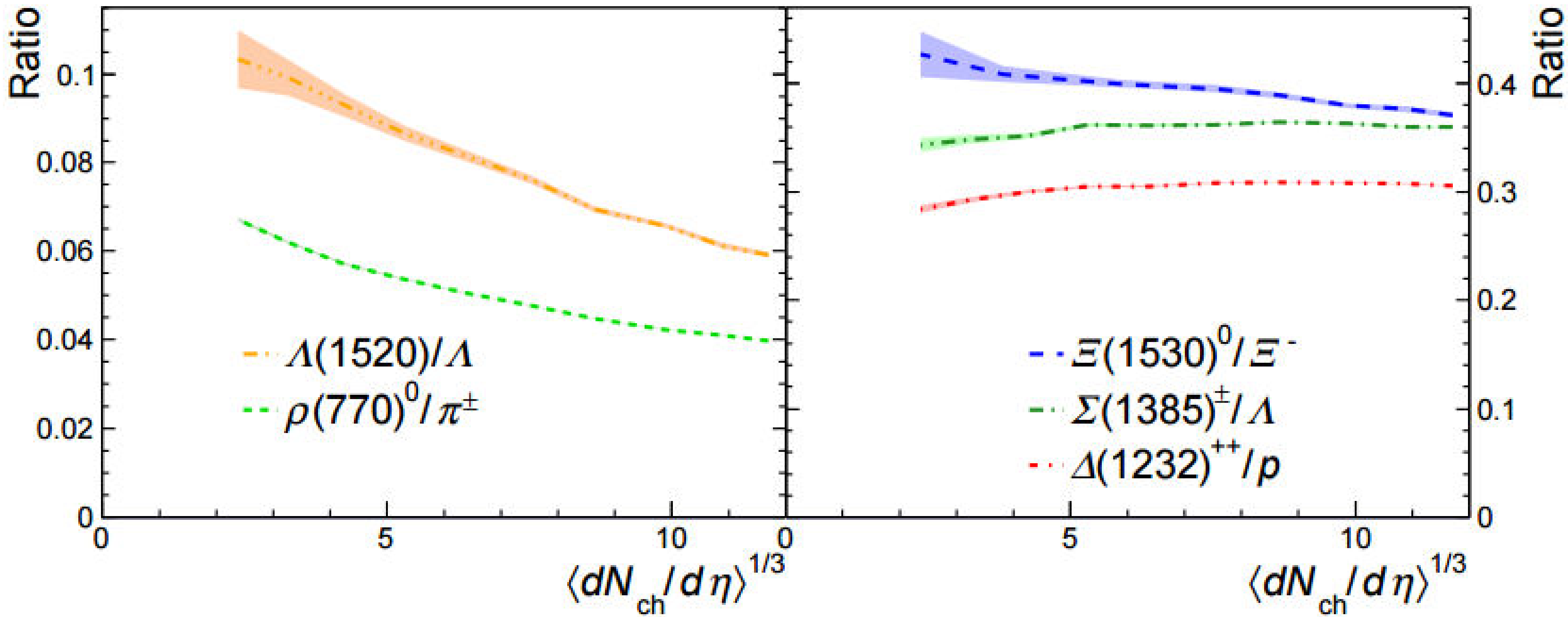

FIG. 13: Ratio of integrated yields $\Sigma(1385)^{\pm}/\Lambda$ and $\rho(770)^0/\pi^{\pm}$ (left) $\Xi(1530)^0/\Xi^-$, $\Sigma(1385)^{\pm}/\Lambda$ and $\Delta(1232)^{++}/p$ (right) for multiple centrality intervals calculated using EPOS3 with UrQMD ON (numerators and denominators are sums of particles and antiparticles). The shaded bands around the EPOS3 curves represent their statistical uncertainties. The theoretical data are plotted as functions of the values of $\langle dN_{ch}/d\eta \rangle^{1/3}$ measured by the ALICE experiment [28] at mid rapidity ($|\eta| < 0.5$).

Nuclear modification factors

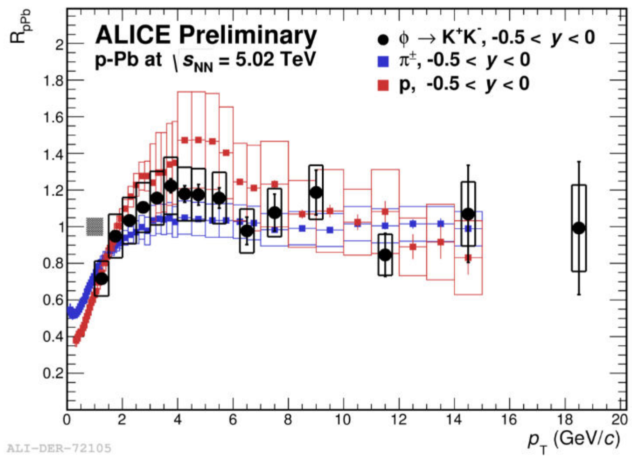

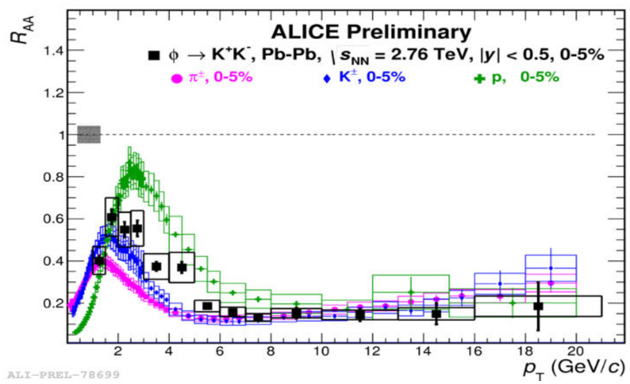

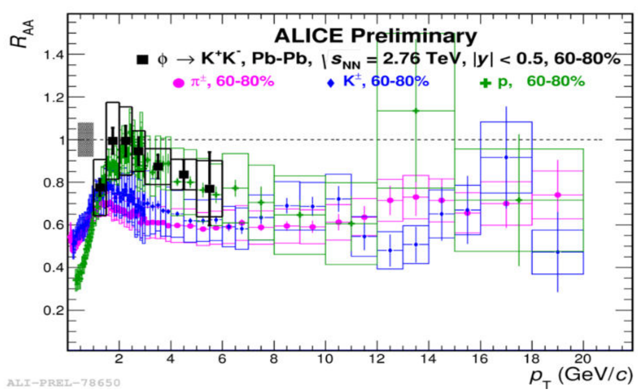

- Nuclear modification factor: $R_{AA}(p_T) = \dfrac{Yield_{A-A}(p_T)}{Yield_{pp}(p_T) \cdot N_{coll}}$
- p-Pb:
  - ✓ R_{pPb} ~ 1 at high p_T > 6-8 GeV/c
  - ✓ Cronin enhancement at intermediate p_T
  - ✓ species dependence of enhancement
    → mass or baryon/meson effect ?
  - ✓ magnitude of enhancement is smaller at the LHC compared to RHIC and SPS
- Pb-Pb:
  - hadrons are similarly suppressed at p_T > 10 GeV/c
  - species dependence of R_{AA} at intermediate p_T
  - R_{AA} of ϕ approaches R_{AA} of proton as centrality evolves from central to peripheral collisions
  - In most central collisions difference of R_{AA} for ϕ and p is governed by difference of pp references (p/ϕ ratio is flat)